

Computation of the one-loop spectral QCD running coupling using covariant spectral regularization

John Mashford

School of Mathematics and Statistics
University of Melbourne, Victoria 3010, Australia
E-mail: mashford@unimelb.edu.au

May 21, 2024

Contents

1	Introduction	2
2	Covariant spectral regularization	5
3	Spectral QCD vacuum polarization	6
3.1	The quark fermion bubble	6
3.2	The gluon bubble	10
3.3	The four-point gluon bubble	18
4	The momentum space spectral QCD running coupling	18
4.1	Computation of the Feynman amplitudes $\mathcal{M}^{(\text{tree})}$ and $\mathcal{M} = \mathcal{M}^{(\text{tree})} + \mathcal{M}^{(\text{vp})}$	19
4.2	Computation of the quantity $\Gamma = \Gamma(q)$ such that $\mathcal{M} = \Gamma \mathcal{M}^{(\text{tree})}$. . .	22
4.3	Computation of the momentum space QCD coupling $q \mapsto g_s(q)$	23
5	The position space spectral QCD running coupling	25

6	Comparison of the spectral QCD running coupling with CERN data	28
7	Freezing of $\alpha_s(\tau)$ as energy $\tau \rightarrow 0$	32
8	Conclusion	32

Abstract

In this paper the spectral QCD vacuum polarization tensor is computed in order to determine and display the (one-loop) spectral QCD running coupling. Through an application of the technique we call covariant spectral regularization the densities associated with the quark and gluon bubbles are computed without requiring renormalization and hence the spectral QCD vacuum polarization tensor is determined. We explain why we think these computations are sufficient to determine the QCD running coupling. It is found that the position space spectral QCD running coupling is an analytic function which does not manifest a Landau pole, but instead it manifests what might be called a “Landau peak”, and has the property known as “freezing of α_s ” in the infrared.

Keywords: QCD; Renormalization and Regularization; Specific QCD Phenomenology; Beyond Standard Model

1 Introduction

The strong force coupling, like the coupling of all the forces of nature, “runs” with collision energy, that being the inverse of the distance to which a target is probed. The couplings of the gravitational, electromagnetic and weak forces are known to great accuracy but the coupling of the strong force (at, e.g., an energy $\tau = m_Z$ where m_Z is the mass of the Z boson) is only known to an accuracy of a world average of about 0.8% [1].

As is well known, the manner in which the strong force coupling “constant” runs is different to, e.g., the manner in which the electromagnetic force coupling constant runs.

The running of the coupling in QCD is an important phenomenon [2, 3, 4] which needs to be taken into account in carrying out calculations in QCD [5]. Since, using standard regularization techniques, the bare coupling is infinite, one must use the finite running coupling in QCD calculations.

The running fine structure constant α_s in QCD can be determined experimentally in a number of ways including deep inelastic scattering, τ decay and

hadron-hadron scattering [3, 1]. In addition it can be determined from lattice gauge theory computations [6]. In all cases its determination involves theoretical QCD calculations involving renormalization. The principal reason for this is that, unlike the case of, e.g., electrons in QED, free quarks have not been observed (except, possibly, in quark-gluon plasma) and the coupling must be inferred from the interactions of quarks bound in hadrons and calculable consequences, and the currently accepted calculation technique involves renormalization.

As a result of asymptotic freedom the behavior of α_s in the perturbative domain is known. However there are, in the literature, a number of different choices for α_s in the non-perturbative domain. “There is no single, agreed prescription for defining an IR completion of QCD’s running coupling” [7], “The optimal choice of the definition of $\alpha_s(Q^2)$ at all scales is an unsettled question” [8].

In QCD the running coupling is not an observable but, in the high energy domain where, due to asymptotic freedom [9, 10] $\alpha_s \ll 1$ so perturbative QCD (pQCD) is applicable, observables are calculated from α_s by expanding to n th order a series in α_s [11]. Thus α_s serves as an intermediate quantity between observables. In the low energy domain analytic expressions based on pQCD are, in various ways, supplemented with non-perturbative terms [8].

The current standard method of computing the QCD running coupling in the high energy domain involves the use of the renormalization method in pQCD. One of the main problems met with in pQCD, in fact in the use of renormalization in general, is the difficulty with setting the renormalization scale μ_r , which arises through the “dimensional transmutation” property of the renormalization method. Only after the renormalization scale has been set can predictions for physical observables be obtained. In the usual method a single μ_r is simply guessed at, and its value is then varied over an arbitrary range [12]. This procedure is *ad hoc* and contradicts renormalization scheme (RS) invariance. Two approaches to getting around this problem are the principle of maximum conformality (PMC) [12] and the Brodsky-Lepage-Mackenzie (BLM) approach [13].

The methods for setting the renormalization scale and defining the running coupling such as the PMC and the BLM approaches are all formulated in the context of the renormalization group (RG) involving the RG equations (RGE) [14, 15, 16]. The RGE predict a singularity, or divergence, in the running coupling called the Landau pole which, for QCD, is estimated to occur at an

energy of the order of a few hundred MeV. Such a divergence is unphysical, it has not been observed either experimentally or in lattice simulations.

Binosi *et al.* [17] describe a process independent running coupling $\hat{\alpha}_{\text{PI}}$ defined by interlacing two functions, one defined in the perturbative domain $k^2 \gg m_0^2$ and the other defined in the nonperturbative domain $k^2 \ll m_0^2$ where $m_0 \approx m_p/2$ ($m_p =$ mass of the proton) involving interpolation of RG continuum and/or lattice QCD calculations using a Padé approximant. $\hat{\alpha}_{\text{PI}}$ coincides closely at low energy with the well known effective charge candidate α_{g_1} defined via the Bjorken sum rule in terms of proton and neutron structure functions which are determined experimentally.

We have developed a method of regularization for QFT which we called spectral regularization and which is described in Refs. [18, 19, 20, 21, 22] and briefly discussed in the next section. We now call this technique covariant spectral regularization in order to distinguish it from other techniques called “spectral regularization”.

Covariant spectral regularization is not associated with any form of divergence, renormalization is not required and one may obtain an expression for the QCD running coupling $\alpha_s(\tau)$ as a function of CM energy τ which does not require the setting of a renormalization scale μ_r .

Peskin and Schroeder [23] in Chapter 6.2 on radiative corrections write in paragraph 2 on page 185 that, for QED, the vertex correction and electron self-energy diagrams represent corrections to an electron response to a given applied field while the vacuum polarization diagram should be considered to be a correction to the electromagnetic field itself. We consider the analogue of this statement to be the case for QCD when analyzed using spectral regularization. Thus we consider the QCD coupling to be determined by the dressed gluon propagator.

Use of the renormalization method in QCD generally requires counterterms which must be obtained from a number of diagrams such as the vacuum polarization, the electron self-energy and the vertex correction diagrams. If one uses the pinch technique in combination with the background field method (PT+BFM) [17] then the gluon polarization function captures all the required features of the renormalization group and hence the UV behavior of the QCD running coupling.

If covariant spectral regularization is used then, since renormalization is not involved, there are no counterterms or the setting of a renormalization scale, the RGE method is not applicable and, we propose, the QCD running coupling

can be determined from (that is, defined to be obtained from) the behavior of the dressed gluon propagator (i.e. from vacuum polarization). We will call the QCD running coupling obtained in this manner (in particular the one-loop case) the spectral QCD running coupling and will, in this paper, be considering its properties.

We will present a method for determining the spectral QCD running coupling based on the relationship between the tree level Feynman amplitude $\mathcal{M}^{(\text{tree})}$ and a total Feynman amplitude $\mathcal{M} = \mathcal{M}^{(\text{tree})} + \mathcal{M}^{(\text{vp})}$ made up of the tree level and the one-loop spectral vacuum polarization Feynman amplitudes for the $u\bar{d} \rightarrow u\bar{d}$ quark scattering process.

Our computations apply at all energies. There is no distinction between perturbative domain and non-perturbative domain. No input of experimental or lattice simulation data (other than the quark masses) is required.

2 Covariant spectral regularization

Covariant spectral regularization has been applied to all the (one-loop) classical tests of QED radiative correction and produces the same results as Pauli-Villars and dimensional regularization/renormalization, (though the technique is applicable to cases where the Feynman diagram has an arbitrary number of loops).

Covariant spectral regularization is based on the technique described in Ref. [18] and the use of the spectral calculus described in Ref. [19].

In Ref. [21] we use covariant spectral regularization to compute the QED vacuum polarization tensor and then use this to compute the Uehling potential function and the Uehling contribution to the Lamb shift for the H atom.

In Ref. [22] we use covariant spectral regularization to compute the vertex function for QED at arbitrary (on shell) values of its arguments in the t channel and the s channel. The low energy and low momenta limit of this function in the t channel is used to compute the one-loop contribution to the anomalous magnetic moment of the electron and the result agrees with Schwinger's classical result. We also use the vertex function in the s channel to compute the leading order vertex correction contribution to the high energy limit of the cross section for the process $e^+e^- \rightarrow \gamma \rightarrow \mu^+\mu^-$ and the result agrees with the textbook result for the cross section for this process [24]. In the textbook computation of this cross section renormalization is used to cancel UV divergence and soft photon final state radiation is used to cancel IR divergence. Our computation

of this cross section does not use renormalization to cancel UV divergence or soft photon final state radiation to cancel IR divergence, since there are no divergences, neither UV nor IR.

Thus we have used covariant spectral regularization on all the classical tests of QED radiative corrections and our results agree with the classical results. While the classical calculations use complicated arguments to negotiate divergences, covariant spectral regularization does not involve divergence of any sort.

In the present paper we use covariant spectral regularization to compute the spectral QCD vacuum polarization tensor and then use this to compute the spectral QCD running coupling.

3 Spectral QCD vacuum polarization

We construct the spectral QCD vacuum polarization tensor $\Pi^{(\text{vp})}$ as

$$\Pi^{(\text{vp})} = \Pi^{(q)} + \Pi^{(g)} + \Pi^{(4)},$$

where $\Pi^{(q)}$ is associated with the quark fermion bubble diagram, $\Pi^{(g)}$ is associated with the gluon bubble diagram and $\Pi^{(4)}$ is associated with the four-point gluon bubble diagram.

We do not include a diagram for “ghosts”. Schwartz (2018 [24], p. 508) writes “That we need these ghosts is a horrible consequence of the Lagrangian formulation of field theory”. Our formulation of field theory is not based on Lagrangians but rather on $U(2, 2)$ covariance (in locally conformally flat space-time X) which gives rise to $U(1) \times SU(2) \times SU(3)$ covariance (in the tangent space $T_x X$) [20, 25]. Therefore we do not “believe in ghosts” in this context.

We now proceed to compute $\Pi^{(q)}$ and $\Pi^{(g)}$ using spectral regularization. In these computations $\Pi^{(q)}$ and $\Pi^{(g)}$ are first represented as (Lorentz covariant) tensor valued measures on Minkowski space (which is isomorphic to $T_x X$) and then spectral calculus [19] is used to compute densities which exactly generate these measures. These densities are functions which can be used for $\Pi^{(q)}$ and $\Pi^{(g)}$ in calculations involving $\Pi^{(\text{vp})}$.

We also show that $\Pi^{(4)}$ vanishes.

3.1 The quark fermion bubble

The quark fermion bubble is shown in Fig. 1. The contribution of this bubble

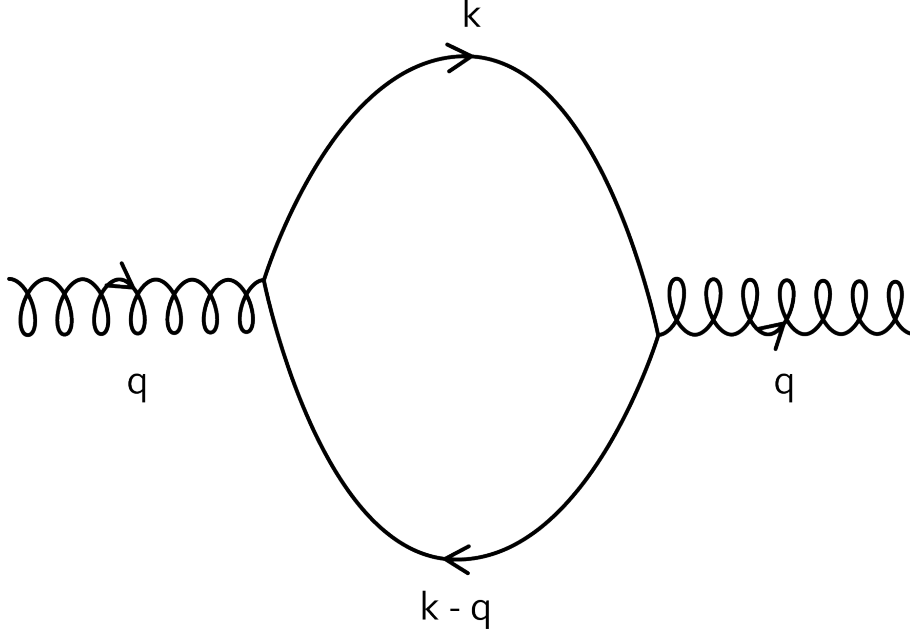


Figure 1: Quark bubble

to the QCD vacuum polarization is (c.f. Schwartz, 2018 [24], p. 517)

$$\begin{aligned} \Pi^{(q)ab\mu\nu}(q) &= -g_s^2 \text{Tr}(T^a T^b) \int \frac{dk}{(2\pi)^4} \frac{1}{(q-k)^2 - m^2 + i\epsilon} \frac{1}{k^2 - m^2 + i\epsilon} \\ &\quad \text{Tr}[\gamma^\mu(\not{k} - \not{q} + m)\gamma^\nu(\not{k} + m)]. \end{aligned} \quad (1)$$

Therefore since

$$\text{Tr}(T^a T^b) = \frac{1}{2} \delta^{ab}, \quad (2)$$

we have

$$\Pi^{(q)ab\mu\nu}(q) = \frac{1}{2} g_s^2 \delta^{ab} \Pi^{(q)\mu\nu}(q), \quad (3)$$

where

$$\Pi^{(q)\mu\nu}(q) = - \int \frac{dk}{(2\pi)^4} \frac{1}{(q-k)^2 - m^2 + i\epsilon} \frac{1}{k^2 - m^2 + i\epsilon} \text{Tr}[\gamma^\mu(\not{k} - \not{q} + m)\gamma^\nu(\not{k} + m)].$$

In line with the work of Refs. [20, 21] suppose (“pretend”) that $\Pi^{(q)\mu\nu}$ existed pointwise and then we can compute (formally) the measure associated with the “function”

$$q \mapsto \Pi^{\mu\nu}(q) = - \int \frac{1}{(q-k)^2 - m^2 + i\epsilon} \frac{1}{k^2 - m^2 + i\epsilon} \text{Tr}[\gamma^\mu(\not{k} - \not{q} + m)\gamma^\nu(\not{k} + m)] dk,$$

as follows. Let $\mathcal{B}_0(\mathbf{R}^4)$ denote the set of relatively compact Borel subsets of \mathbf{R}^4 . Now let $\Gamma \in \mathcal{B}_0(\mathbf{R}^4)$. Then

$$\begin{aligned}
\Pi^{\mu\nu}(\Gamma) &= \int_{\Gamma} \Pi^{\mu\nu}(q) dq \\
&= \int \chi_{\Gamma}(q) \Pi^{\mu\nu}(q) dq \\
&= - \int \chi_{\Gamma}(q) \frac{1}{(q-k)^2 - m^2 + i\epsilon} \frac{1}{k^2 - m^2 + i\epsilon} \\
&\quad \text{Tr}[\gamma^{\mu}(\not{k} - \not{q} + m)\gamma^{\nu}(\not{k} + m)] dk dq \\
&= - \int \chi_{\Gamma}(q) \frac{1}{(q-k)^2 - m^2 + i\epsilon} \frac{1}{k^2 - m^2 + i\epsilon} \\
&\quad \text{Tr}[\gamma^{\mu}(\not{k} - \not{q} + m)\gamma^{\nu}(\not{k} + m)] dq dk \\
&= \int \chi_{\Gamma}(q+k) \frac{1}{q^2 - m^2 + i\epsilon} \frac{1}{k^2 - m^2 + i\epsilon} \\
&\quad \text{Tr}[\gamma^{\mu}(\not{q} - m)\gamma^{\nu}(\not{k} + m)] dq dk \\
&= -\pi^2 \int \chi_{\Gamma}(q+k) \text{Tr}[\gamma^{\mu}(\not{q} - m)\gamma^{\nu}(\not{k} + m)] \Omega_m(dq)\Omega_m(dk),
\end{aligned}$$

where, for any set Γ , χ_{Γ} denotes the characteristic function of Γ defined by

$$\chi_{\Gamma}(q) = \begin{cases} 1 & \text{if } q \in \Gamma, \\ 0 & \text{otherwise,} \end{cases} \quad (4)$$

and we have used the result [19, 20, 21, 25] that

$$\frac{1}{q^2 - m^2 + i\epsilon} \rightarrow -\pi i \Omega_m^{\pm}(q), \quad (5)$$

in which, for $m \geq 0$, Ω_m^{\pm} denotes the standard Lorentz invariant measure on the mass shell $H_m^{\pm} = \pm\{q \in \mathbf{R}^4 : q^2 = m^2, q^0 > 0\}$ [19, 20, 21].

Therefore the measure associated with $\Pi^{(q)\mu\nu}$ is

$$\Pi^{(q)\mu\nu}(\Gamma) = -\frac{1}{16\pi^2} \int \chi_{\Gamma}(q+k) \text{Tr}[\gamma^{\mu}(\not{q} - m)\gamma^{\nu}(\not{k} + m)] \Omega_m(dq)\Omega_m(dk). \quad (6)$$

$\Pi^{(q)\mu\nu}$ is analogous to the measure associated with the QED vacuum polarization tensor and it can be shown [21, 20] that $\Pi^{(q)\mu\nu}$ is a causal tempered Borel measure on Minkowski space and is associated with a density $\Pi^{(q)\mu\nu}$ given by

$$\Pi^{(q)\mu\nu}(q) = (q^2 \eta^{\mu\nu} - q^{\mu} q^{\nu}) \pi^{(q)}(s) = (s^2 \eta^{\mu\nu} - q^{\mu} q^{\nu}) \pi^{(q)}(s), \quad (7)$$

where

$$\pi^{(q)}(s) = -\frac{2}{3\pi}m^3s^{-3}Z(s)(3+2Z(s)^2), \quad (8)$$

$s = (q^2)^{\frac{1}{2}}$ and

$$Z(s) = \begin{cases} \left(\frac{s^2}{4m^2} - 1\right)^{\frac{1}{2}} & \text{if } s \geq 2m, \\ 0 & \text{otherwise.} \end{cases} \quad (9)$$

In the spacelike domain we have, following [21], since $\pi^{(q)}$ is odd in s , that $\Pi^{(q)}$ is given by

$$\Pi^{(q)\mu\nu}(q) = -(Q^2\eta^{\mu\nu} - q^\mu q^\nu)\pi^{(q)}(Q), \quad (10)$$

where $Q = (-q^2)^{\frac{1}{2}}$. Therefore, by Eq. 3

$$\Pi^{(q)ab\mu\nu}(q) = \frac{1}{3\pi}g_s^2\delta^{ab}m^3Q^{-3}Z(Q)(3+2Z(Q)^2)(Q^2\eta^{\mu\nu} - q^\mu q^\nu),$$

where $Q = (-q^2)^{\frac{1}{2}}$.

Now there are six quark types with flavors $f_q = u, d, s, c, b, t$ and masses $m_q \in \{m_1, \dots, m_6\}$ say. Therefore we take the total quark bubble contribution to the hadronic vacuum polarization tensor to be given by

$$\Pi^{(q,\text{tot})ab\mu\nu}(q) = \sum_{k=1}^6 \Pi^{(q)ab\mu\nu}(m_k, q), \quad (11)$$

where

$$\Pi^{(q)ab\mu\nu}(m, q) = \frac{1}{3\pi}g_s^2\delta^{ab}m^3Q^{-3}Z(m, Q)(3+2Z(m, Q)^2)(Q^2\eta^{\mu\nu} - q^\mu q^\nu), \quad (12)$$

in which

$$Z(m, Q) = \begin{cases} \left(\frac{Q^2}{4m^2} - 1\right)^{\frac{1}{2}} & \text{if } Q \geq 2m, \\ 0 & \text{otherwise} \end{cases} \quad (13)$$

and $Q = (-q^2)^{\frac{1}{2}}$.

It is not necessary to specify which quarks are ‘‘active’’ at any given energy. This is automatically worked out in Eq. 12 by the value determined by that equation corresponding to any given quark type at any given energy.

$\Pi^{(q)}$ stands for the six different quark bubble diagrams that need to be considered when computing the total vacuum polarization.

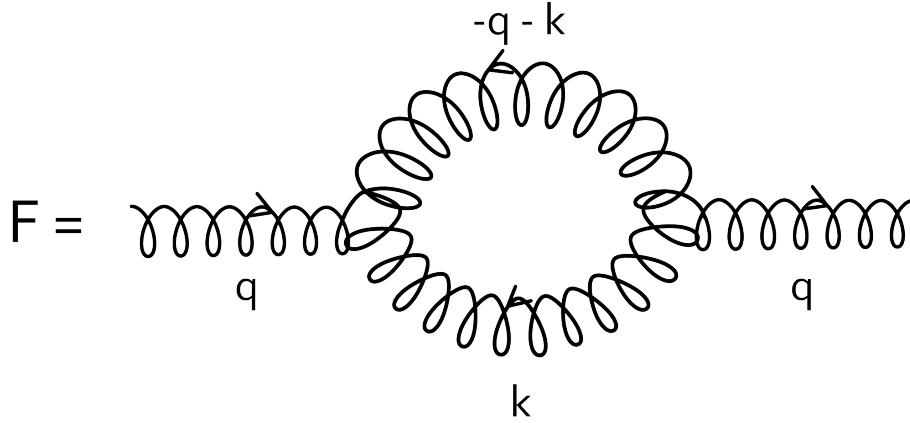


Figure 2: gluon bubble diagram F

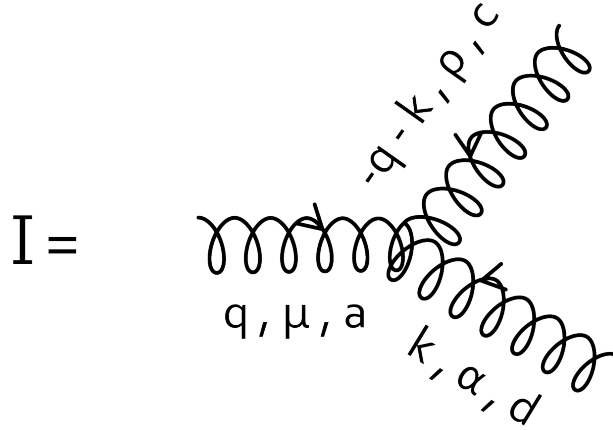


Figure 3: gluon bubble diagram I

3.2 The gluon bubble

The contribution from the gluon bubble is

$$\begin{aligned}
 \Pi^{(g)ab\mu\nu}(q) &= \frac{1}{2} \int \frac{dk}{(2\pi)^4} \frac{-i}{k^2 + i\epsilon} \frac{-i}{(k+q)^2 + i\epsilon} F^{ab\mu\nu}(q, k) \\
 &= -\frac{1}{2} \int \frac{dk}{(2\pi)^4} \frac{1}{k^2 + i\epsilon} \frac{1}{(k+q)^2 + i\epsilon} F^{ab\mu\nu}(q, k), \quad (14)
 \end{aligned}$$

where $F^{ab\mu\nu}$ is defined by the Feynman diagram F shown in Fig. 2. F is constructed from the diagrams I and II shown in Figs. 3 and 4.

The overall factor of $\frac{1}{2}$ is a symmetry factor required because the gluons are their own antiparticle (Schwartz, 2018 [24], p. 518).

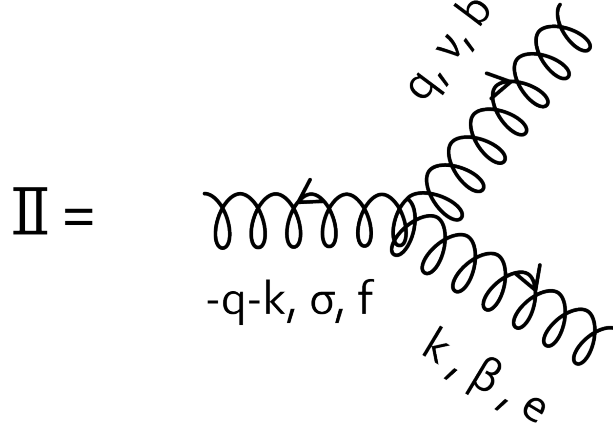


Figure 4: gluon bubble diagram II

Using the QCD Feynman rules (Schwartz, 2018 [24], p. 510) we have

$$I^{cad\rho\mu\alpha}(q, k) = g_s f^{cad} (\eta^{\rho\mu} (-2q - k)^\alpha + \eta^{\mu\alpha} (q - k)^\rho + \eta^{\alpha\rho} (2k + q)^\mu),$$

$$II^{bf\nu\sigma\beta}(q, k) = g_s f^{bf\nu\sigma\beta} (\eta^{\nu\sigma} (-2q - k)^\beta + \eta^{\sigma\beta} (2k + q)^\nu + \eta^{\beta\nu} (q - k)^\sigma),$$

and

$$F^{ab\mu\nu}(q, k) = \delta^{cf} \delta^{de} \eta^{\rho\sigma} \eta^{\alpha\beta} I^{cad\rho\mu\alpha}(q, k) II^{bf\nu\sigma\beta}(q, k).$$

Now

$$\delta^{cf} \delta^{de} g_s f^{cad} g_s f^{bf\nu\sigma\beta} = g_s^2 f^{cad} f^{bcd} = -g_s^2 f^{acd} f^{bcd} = -3g_s^2 \delta^{ab}.$$

Therefore

$$F^{ab\mu\nu}(q, k) = -3g_s^2 \delta^{ab} N^{\mu\nu}(q, k),$$

where

$$N^{\mu\nu}(q, k) = [\eta^{\mu\alpha} (q - k)^\rho + \eta^{\alpha\rho} (q + 2k)^\mu - \eta^{\rho\mu} (k + 2q)^\alpha] \eta_{\alpha\beta} \eta_{\rho\sigma} \\ \times [\eta^{\nu\beta} (q - k)^\sigma + \eta^{\beta\sigma} (2k + q)^\nu - \eta^{\sigma\nu} (2q + k)^\beta].$$

We compute (formally) the measure $\Xi^{\mu\nu}$ associated with the “function” $q \mapsto$

$\Xi^{\mu\nu}(q) = \int \frac{1}{k^2+i\epsilon} \frac{1}{(k+q)^2+i\epsilon} N^{\mu\nu}(q, k) dk$ as follows.

$$\begin{aligned}
\Xi^{\mu\nu}(\Gamma) &= \int_{\Gamma} \Pi^{\mu\nu}(q) dq \\
&= \int \chi_{\Gamma}(q) \Pi^{\mu\nu}(q) dq \\
&= \int \chi_{\Gamma}(q) \frac{1}{k^2+i\epsilon} \frac{1}{(k+q)^2+i\epsilon} N^{\mu\nu}(q, k) dk dq \\
&= \int \chi_{\Gamma}(q) \frac{1}{k^2+i\epsilon} \frac{1}{(k+q)^2+i\epsilon} N^{\mu\nu}(q, k) dq dk \\
&= \int \chi_{\Gamma}(q-k) \frac{1}{k^2+i\epsilon} \frac{1}{q^2+i\epsilon} N^{\mu\nu}(q-k, k) dq dk \\
&= \int \chi_{\Gamma}(q+k) \frac{1}{k^2+i\epsilon} \frac{1}{q^2+i\epsilon} N^{\mu\nu}(q+k, -k) dq dk \\
&= -\pi^2 \int \chi_{\Gamma}(q+k) N^{\mu\nu}(q+k, -k) \Omega_0(dq) \Omega_0(dk)
\end{aligned}$$

For each $\mu, \nu \in \{0, 1, 2, 3\}$ define $M^{\mu\nu} : \mathbf{R}^4 \times \mathbf{R}^4 \rightarrow \mathbf{R}$ by

$$M^{\mu\nu}(q, k) = N^{\mu\nu}(q+k, -k). \quad (15)$$

Then

$$\Xi^{\mu\nu}(\Gamma) = -\pi^2 \int \chi_{\Gamma}(q+k) M^{\mu\nu}(q, k) \Omega_0(dq) \Omega_0(dk),$$

and therefore

$$\Pi^{(g)ab\mu\nu}(\Gamma) = -\frac{3}{32\pi^2} g_s^2 \delta^{ab} \int \chi_{\Gamma}(q+k) M^{\mu\nu}(q, k) \Omega_0(dq) \Omega_0(dk),$$

where

$$\begin{aligned}
M^{\mu\nu}(q, k) &= N^{\mu\nu}(q + k, -k) \\
&\eta_{\alpha\beta}\eta_{\rho\sigma}[\eta^{\mu\alpha}(q + 2k)^\rho + \eta^{\alpha\rho}(q - k)^\mu - \eta^{\rho\mu}(2q + k)^\alpha] \\
&\times [\eta^{\nu\beta}(q + 2k)^\sigma + \eta^{\beta\sigma}(q - k)^\nu - \eta^{\sigma\nu}(2q + k)^\beta] \\
&= \eta_{\alpha\beta}\eta_{\rho\sigma}\eta^{\mu\alpha}\eta^{\nu\beta}(q + 2k)^\rho(q + 2k)^\sigma \\
&+ \eta_{\alpha\beta}\eta_{\rho\sigma}\eta^{\mu\alpha}\eta^{\beta\sigma}(q + 2k)^\rho(q - k)^\nu \\
&- \eta_{\alpha\beta}\eta_{\rho\sigma}\eta^{\mu\alpha}\eta^{\sigma\nu}(q + 2k)^\rho(2q + k)^\beta \\
&+ \eta_{\alpha\beta}\eta_{\rho\sigma}\eta^{\alpha\rho}\eta^{\nu\beta}(q - k)^\mu(q + 2k)^\sigma \\
&+ \eta_{\alpha\beta}\eta_{\rho\sigma}\eta^{\alpha\rho}\eta^{\beta\sigma}(q - k)^\mu(q - k)^\nu \\
&- \eta_{\alpha\beta}\eta_{\rho\sigma}\eta^{\alpha\rho}\eta^{\sigma\nu}(q - k)^\mu(2q + k)^\beta \\
&- \eta_{\alpha\beta}\eta_{\rho\sigma}\eta^{\rho\mu}\eta^{\nu\beta}(2q + k)^\alpha(q + 2k)^\sigma \\
&- \eta_{\alpha\beta}\eta_{\rho\sigma}\eta^{\rho\mu}\eta^{\beta\sigma}(2q + k)^\alpha(q - k)^\nu \\
&+ \eta_{\alpha\beta}\eta_{\rho\sigma}\eta^{\rho\mu}\eta^{\sigma\nu}(2q + k)^\alpha(2q + k)^\beta \\
&= (q + 2k)^2\eta^{\mu\nu} \\
&+ (q + 2k)^\mu(q - k)^\nu \\
&- (2q + k)^\mu(q + 2k)^\nu \\
&+ (q - k)^\mu(q + 2k)^\nu \\
&+ 4(q - k)^\mu(q - k)^\nu \\
&- (q - k)^\mu(2q + k)^\nu \\
&- (q + 2k)^\mu(2q + k)^\nu \\
&- (2q + k)^\mu(q - k)^\nu \\
&+ (2q + k)^2\eta^{\mu\nu} \\
&= (5q^2 + 5k^2 + 8q \cdot k)\eta^{\mu\nu} + q^\mu q^\nu + 2k^\mu q^\nu - q^\mu k^\nu - 2k^\mu k^\nu - 2q^\mu q^\nu - k^\mu q^\nu - 4q^\mu k^\nu \\
&- 2k^\mu k^\nu + q^\mu q^\nu - k^\mu q^\nu + 2q^\mu k^\nu - 2k^\mu k^\nu + 4q^\mu q^\nu - 4k^\mu q^\nu - 4q^\mu k^\nu + 4k^\mu k^\nu \\
&- 2q^\mu q^\nu - q^\mu k^\nu + 2k^\mu q^\nu + k^\mu k^\nu - 2q^\mu q^\nu - 4k^\mu q^\nu - q^\mu k^\nu - 2k^\mu k^\nu \\
&- 2q^\mu q^\nu - k^\mu q^\nu + 2q^\mu k^\nu + k^\mu k^\nu \\
&= (5q^2 + 5k^2 + 8q \cdot k)\eta^{\mu\nu} - 2q^\mu q^\nu - 2k^\mu k^\nu - 7q^\mu k^\nu - 7k^\mu q^\nu.
\end{aligned}$$

It is straightforward to show that $\Pi^{(g)ab\mu\nu}$ is a well defined Borel measure on Minkowski space \mathbf{R}^4 . Write

$$\Pi^{(g)ab\mu\nu}(\Gamma) = \Pi^{(g)ab}\Pi^{(g)\mu\nu}(\Gamma), \quad (16)$$

where

$$\Pi^{(g)ab} = -\frac{3}{32\pi^2}g_s^2\delta^{ab},$$

and

$$\Pi^{(g)\mu\nu}(\Gamma) = \int \chi_\Gamma(q+k)M^{\mu\nu}(q,k)\Omega_0(dq)\Omega_0(dk).$$

Using the Lorentz invariance of Ω_0 , for any $\Lambda \in O(1,3)^{\uparrow+}$, $\Gamma \in \mathcal{B}_0(\mathbf{R}^4)$

$$\begin{aligned}\Pi^{(g)\mu\nu}(\Lambda\Gamma) &= \int \chi_{\Lambda\Gamma}(q+k)M^{\mu\nu}(q,k)\Omega_0(dq)\Omega_0(dk), \\ &= \int \chi_\Gamma(\Lambda^{-1}q+\Lambda^{-1}k)M^{\mu\nu}(q,k)\Omega_0(dq)\Omega_0(dk), \\ &= \int \chi_\Gamma(q+k)M^{\mu\nu}(\Lambda q,\Lambda k)\Omega_0(dq)\Omega_0(dk).\end{aligned}$$

But we have

$$\begin{aligned}M^{\mu\nu}(\Lambda q,\Lambda k) &= \eta^{\mu\nu}(5(\Lambda q)^2+5(\Lambda k)^2+8(\Lambda q)\cdot(\Lambda k))-2(\Lambda q)^\mu(\Lambda q)^\nu- \\ &\quad 2(\Lambda k)^\mu(\Lambda k)^\nu-7(\Lambda q)^\mu(\Lambda k)^\nu-7(\Lambda k)^\mu(\Lambda q)^\nu \\ &= \Lambda^\mu{}_\rho\Lambda^\nu{}_\sigma(\eta^{\rho\sigma}(5q^2+5k^2+8q\cdot k)-2q^\rho q^\sigma- \\ &\quad 2k^\rho k^\sigma-7q^\rho k^\sigma-7k^\rho q^\sigma) \\ &= \Lambda^\mu{}_\rho\Lambda^\nu{}_\sigma M^{\rho\sigma}(q,k).\end{aligned}$$

Therefore

$$\Pi^{(g)\mu\nu}(\Lambda\Gamma) = \Lambda^\mu{}_\rho\Lambda^\nu{}_\sigma\Pi^{(g)\rho\sigma}(\Gamma), \forall \Lambda \in O(1,3)^{\uparrow+}, \Gamma \in \mathcal{B}_0(\mathbf{R}^4), \quad (17)$$

and so $\Pi^{\mu\nu}$ is Lorentz covariant in the sense defined in Ref. [21].

By a similar argument to that used in Ref. [19] the support of $\Pi^{(g)\mu\nu}$ satisfies $\text{supp}(\Pi^{(g)\mu\nu}) \subset \{q \in \mathbf{R}^4 : q^2 \geq 0, q^0 \geq 0\}$. Thus $\Pi^{(g)\mu\nu}$ is causal. We will now show, using the spectral calculus, [18, 19, 21, 26] that $\Pi^{(g)\mu\nu}$ has a spectral representation

$$\Pi^{(g)\mu\nu}(\Gamma) = \int_{m'=0}^{\infty} q^2 \eta^{\mu\nu} \Omega_{m'}(\Gamma) \sigma_1(dm') + \int_{m'=0}^{\infty} q^\mu q^\nu \Omega_{m'}(\Gamma) \sigma_2(dm'), \quad (18)$$

where the spectral measures σ_1, σ_2 are continuous functions. Let $a, b \in \mathbf{R}, 0 <$

$a < b$. We have

$$\begin{aligned}
g^{\mu\nu}(a, b, \epsilon) &= \Pi^{(g)\mu\nu}(\Gamma(a, b, \epsilon)) \\
&= \int \chi_{\Gamma(a, b, \epsilon)}(q + k) M^{\mu\nu}(q, k) \Omega_0(dk) \Omega_0(dq) \\
&\approx \int \chi_{(a, b)}(|\vec{q}| + |\vec{k}|) \chi_{B_\epsilon(\vec{0})}(\vec{q} + \vec{k}) M^{\mu\nu}((|\vec{q}|, \vec{q}), (|\vec{k}|, \vec{k})) \frac{d\vec{k}}{|\vec{k}|} \frac{d\vec{q}}{|\vec{q}|} \\
&= \int \chi_{(a, b)}(|\vec{q}| + |\vec{k}|) \chi_{B_\epsilon(\vec{0}) - \vec{q}}(\vec{k}) M^{\mu\nu}((|\vec{q}|, \vec{q}), (|\vec{k}|, \vec{k})) \frac{d\vec{k}}{|\vec{k}|} \frac{d\vec{q}}{|\vec{q}|} \\
&\approx \int \chi_{(a, b)}(2|\vec{q}|) M^{\mu\nu}((|\vec{q}|, \vec{q}), (|\vec{q}|, -\vec{q})) \frac{d\vec{q}}{|\vec{q}|^2} \left(\frac{4}{3}\pi\epsilon^3\right),
\end{aligned}$$

for all $a, b \in \mathbf{R}$ with $0 < a < b$. Now

$$\chi_{(a, b)}(2|\vec{q}|) = 1 \Leftrightarrow 2|\vec{q}| \in (a, b) \Leftrightarrow |\vec{q}| \in \left(\frac{a}{2}, \frac{b}{2}\right).$$

Hence, using spherical polar coordinates,

$$\begin{aligned}
g_a^{\mu\nu}(b) &= \int_{s=\frac{a}{2}}^{\frac{b}{2}} \int_{\theta=0}^{\pi} \int_{\phi=0}^{2\pi} M^{\mu\nu}((s, s \sin(\theta) \cos(\phi), s \sin(\theta) \sin(\phi), s \cos(\theta)), \\
&\quad (s, -s \sin(\theta) \cos(\phi), -s \sin(\theta) \sin(\phi), -s \cos(\theta))) \sin(\theta) d\phi d\theta ds \left(\frac{4}{3}\pi\right).
\end{aligned}$$

Thus, using the Leibniz integral rule

$$\begin{aligned}
g_a^{\mu\nu}(b) &= \int_{\theta=0}^{\pi} \int_{\phi=0}^{2\pi} M^{\mu\nu}\left(\frac{b}{2}(1, \sin(\theta) \cos(\phi), \sin(\theta) \sin(\phi), \cos(\theta)), \right. \\
&\quad \left. \frac{b}{2}(1, -\sin(\theta) \cos(\phi), -\sin(\theta) \sin(\phi), -\cos(\theta))\right) \sin(\theta) d\phi d\theta \left(\frac{2}{3}\pi\right) \\
&= b^2 \int_{\theta=0}^{\pi} \int_{\phi=0}^{2\pi} M^{\mu\nu}((1, \sin(\theta) \cos(\phi), \sin(\theta) \sin(\phi), \cos(\theta)), \\
&\quad (1, -\sin(\theta) \cos(\phi), -\sin(\theta) \sin(\phi), -\cos(\theta))) \sin(\theta) d\phi d\theta \left(\frac{1}{6}\pi\right),
\end{aligned}$$

where we have used the fact that

$$M(\lambda q, \lambda k) = \lambda^2 M(q, k), \forall \lambda \in \mathbf{R}, q, k \in \mathbf{R}^4.$$

Therefore, since if $q = (1, \sin(\theta) \cos(\phi), \sin(\theta) \sin(\phi), \cos(\theta))$ and $k = (1, -\sin(\theta) \cos(\phi), -\sin(\theta) \sin(\phi), -\cos(\theta))$ then $q^2 = k^2 = 0$, $q \cdot k = 2$ and $k = (k^0, \vec{k}) = (q^0, -\vec{q})$,

we have, for all $i \in \{1, 2, 3\}$

$$\begin{aligned}
M^{ii}(q, k) &= -5q^2 - 5k^2 - 8q \cdot k - 2(q^i)^2 - 2(k^i)^2 - 7q^i k^i - 7k^i q^i \\
&= -16 - 2(q^i)^2 - 2(k^i)^2 + 7(q^i)^2 + 7(k^i)^2 \\
&= -16 + 10(q^i)^2,
\end{aligned}$$

and so

$$\begin{aligned}
g_a^{11'}(b) &= \frac{1}{6}\pi b^2 \int_{\theta=0}^{\pi} \int_{\phi=0}^{2\pi} (-16 + 10 \sin^2(\theta) \cos^2(\phi)) \sin(\theta) d\phi d\theta \\
&= \frac{1}{6}\pi b^2 (-16(4\pi) + 10(\frac{4}{3})\pi) \\
&= -\frac{76}{9}\pi^2 b^2, \\
g_a^{22'}(b) &= \frac{1}{6}\pi b^2 \int_{\theta=0}^{\pi} \int_{\phi=0}^{2\pi} (-16 + 10 \sin^2(\theta) \sin^2(\phi)) \sin(\theta) d\phi d\theta \\
&= \frac{1}{6}\pi b^2 (-16(4\pi) + 10(\frac{4}{3})\pi) \\
&= -\frac{76}{9}\pi^2 b^2, \\
g_a^{33'}(b) &= \frac{1}{6}\pi b^2 \int_{\theta=0}^{\pi} \int_{\phi=0}^{2\pi} (-16 + 10 \cos^2(\theta)) \sin(\theta) d\phi d\theta \\
&= \frac{1}{6}\pi b^2 (2\pi)(-16(2) + 10(\frac{2}{3})) \\
&= -\frac{76}{9}\pi^2 b^2.
\end{aligned}$$

Thus

$$g_a^{ii'}(b) = g_a^{jj'}(b), \forall i, j \in \{1, 2, 3\}, b > a, \quad (19)$$

and as it should from the general theory [26] and

$$g_a^{iii'}(b) = -\frac{76}{9}\pi^2 b^2, \forall i \in \{1, 2, 3\}, b > a. \quad (20)$$

Also

$$g_a^{00'}(b) = \frac{1}{6}\pi b^2 \int_{\theta=0}^{\pi} \int_{\phi=0}^{2\pi} ((5q^2 + 5k^2 + 8q \cdot k) - 2(q^0)^2 - 2(k^0)^2 - 7(q^0)^2 - 7(k^0)^2) \sin(\theta) d\phi d\theta \quad (21)$$

$$\sin(\theta) d\phi d\theta = \frac{1}{6}\pi b^2 (4\pi)(16 - 18) = -\frac{4}{3}\pi^2 b^2.$$

From the general theory (the spectral theory for Lorentz covariant tensor valued

measures [20, 21, 26]) the measure $\Pi^{g\mu\nu}$ is given by

$$\Pi^{(g)\mu\nu}(\Gamma) = \int_{m'=0}^{\infty} \int_{\mathbf{R}^4} \chi_{\Gamma}(q)(\eta^{\mu\nu} q^2 \sigma_1^{(g)}(m') + q^{\mu} q^{\nu} \sigma_2^{(g)}(m')) \Omega_{m'}(dq) dm', \quad (22)$$

where

$$\sigma_1^{(g)}(b) = -\frac{3}{4\pi} \frac{1}{b} g_a^{i i'}(b), \quad i \in \{1, 2, 3\}, \quad (23)$$

$$\sigma_2^{(g)}(b) = \frac{3}{4\pi} \frac{1}{b} g_a^{00'}(b) - \sigma_1(b), \quad (24)$$

and is associated with a density $\Pi^{(g)\mu\nu} : \{q \in \mathbf{R}^4 : q^2 > 0, q^0 > 0\} \rightarrow \mathbf{R}$ given by

$$\Pi^{(g)\mu\nu}(q) = \eta^{\mu\nu} s \sigma_1^{(g)}(s) + q^{\mu} q^{\nu} s^{-1} \sigma_2^{(g)}(s),$$

for $q^2 > 0, q^0 > 0$ where $s = (q^2)^{\frac{1}{2}}$. From Eqns. 20, 21, 23 and 24 we have that

$$\sigma_1^{(g)}(s) = \left(-\frac{3}{4\pi} \frac{1}{s}\right) \left(-\frac{76}{9} \pi^2 s^2\right) = \frac{19}{3} \pi s, \quad \forall s > 0. \quad (25)$$

and

$$\sigma_2^{(g)}(s) = \frac{3}{4\pi} \frac{1}{s} g_a^{00'}(s) - \sigma_1(s) = \left(\frac{3}{4\pi} \frac{1}{s}\right) \left(-\frac{4}{3} \pi^2 s^2\right) - \sigma_1(s), \quad \forall s > 0.$$

Therefore

$$\Pi^{(g)\mu\nu}(q) = \frac{19}{3} \pi s^2 \eta^{\mu\nu} + q^{\mu} q^{\nu} s^{-1} \sigma_2^{(g)}(s). \quad (26)$$

In the spacelike domain, since both σ_1 and σ_2 are odd functions, $\Pi^{(g)\mu\nu} : \{q \in \mathbf{R}^4 : q^2 < 0\} \rightarrow \mathbf{R}$ is given by

$$\Pi^{(g)\mu\nu}(q) = \frac{19}{3} \pi Q^2 \eta^{\mu\nu} + q^{\mu} q^{\nu} Q^{-1} \sigma_2^{(g)}(Q), \quad (27)$$

where $Q = (-q^2)^{\frac{1}{2}}$.

Hence, from Eq. 16

$$\Pi^{(g)ab\mu\nu}(q) = \left(-\frac{3}{32\pi^2} g_s^2 \delta^{ab}\right) \left(\frac{19}{3} \pi Q^2 \eta^{\mu\nu} + Q^{-1} \sigma_2^{(g)}(Q) q^{\mu} q^{\nu}\right) \quad (28)$$

$$= -\frac{19}{32\pi} g_s^2 \delta^{ab} \eta^{\mu\nu} Q^2 - \frac{3}{32\pi^2} g_s^2 \delta^{ab} Q^{-1} \sigma_2^{(g)}(Q) q^{\mu} q^{\nu}, \quad (29)$$

where $Q = (-q^2)^{\frac{1}{2}}$.

3.3 The four-point gluon bubble

The four-point gluon bubble is associated with a function $q \mapsto \Pi^{(4)ab\mu\nu}(q)$ whose value is a constant tensor times the constant “function”

$$f(q) = c \text{ where } c = \int \frac{1}{k^2 + i\epsilon} dk,$$

(Schwartz, 2018 [24], p. 519). We will argue (somewhat formally, since the integral defining c is divergent) that $c = 0$ as follows. Assume that c is finite. Then we have

$$c = \int (k^2 + i\epsilon)^{-1} dk.$$

Make a change of variables $l = \lambda k$ where $\lambda > 0$. Then

$$k = \lambda^{-1}l, dk = \lambda^{-4}dl, k^2 = \lambda^{-2}l^2.$$

Therefore

$$c = \int (\lambda^{-2}l^2 + i\epsilon)^{-1} (\lambda^{-4}dl) = \lambda^{-2} \int (l^2 + i\epsilon)^{-1} dl = \lambda^{-2}c.$$

Since this is true for all $\lambda > 0$ we must have that $c = 0$.

Thus the four-point gluon bubble vanishes.

4 The momentum space spectral QCD running coupling

The method we use is exact and fully relativistic (not an NR approximation). It is not based on approximate solutions to the Lippmann-Schwinger equation (e.g. the Born approximations) and it does not involve the Schwinger-Dyson equation. It applies over the whole range of possible input and output momenta and polarizations. Thus it applies over the whole range of energies, from IR to UV.

To compute the running coupling at one-loop level we compare the process described by the tree level Feynman amplitude $\mathcal{M}^{(\text{tree})}$ with the process described by the Feynman amplitude $\mathcal{M} = \mathcal{M}^{(\text{tree})} + \mathcal{M}^{(\text{vp})}$, where $\mathcal{M}^{(\text{vp})}$ is the one-loop spectral vacuum polarization Feynman amplitude, for quark $u\bar{d}$ scattering.

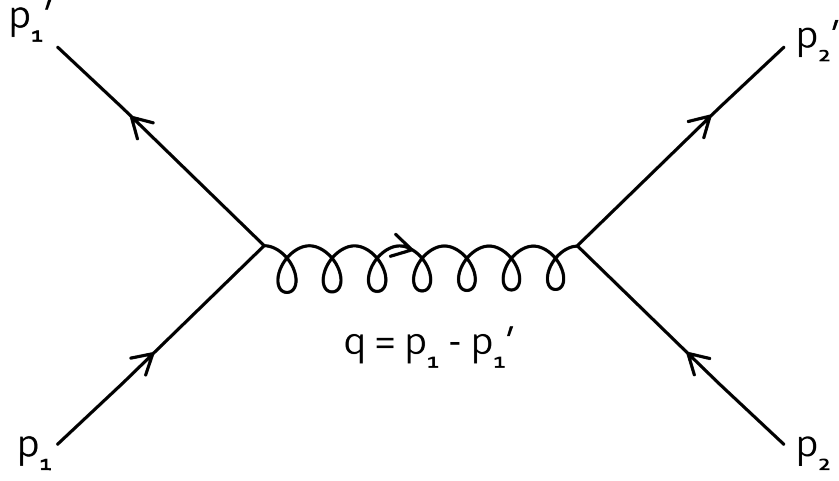


Figure 5: Tree level quark $u\bar{d}$ scattering

4.1 Computation of the Feynman amplitudes $\mathcal{M}^{(\text{tree})}$ and $\mathcal{M} = \mathcal{M}^{(\text{tree})} + \mathcal{M}^{(\text{vp})}$

The tree level process is the process associated with the Feynman diagram given in Fig. 5 and, using the Feynman rules, we have that the tree level Feynman amplitude $\mathcal{M}^{(\text{tree})}$ is given by

$$\begin{aligned}
 i\mathcal{M}_{i_1' i_2' \alpha_1' \alpha_2' i_1 i_2 \alpha_1 \alpha_2}^{(\text{tree})}(p_1', p_2', p_1, p_2) &= \bar{u}(p_1', \alpha_1') i g_s T_{i_1' i_1}^a \gamma^\mu u(p_1, \alpha_1) \quad (30) \\
 &\quad \left(-i \frac{\delta_{ab} \eta_{\mu\nu}}{q^2 + i\epsilon} \right) \\
 &\quad \bar{v}(p_2, \alpha_2) i g_s T_{i_2 i_2'}^b \gamma^\nu v(p_2', \alpha_2'),
 \end{aligned}$$

where u and v are the Dirac spinors defined by

$$\begin{aligned}
 u(p, \alpha) &= \begin{pmatrix} (p \cdot \sigma)^{\frac{1}{2}} e_\alpha \\ (p \cdot \bar{\sigma})^{\frac{1}{2}} e_\alpha \end{pmatrix}, \\
 v(p, \alpha) &= \begin{pmatrix} (p \cdot \sigma)^{\frac{1}{2}} e_\alpha \\ -(p \cdot \bar{\sigma})^{\frac{1}{2}} e_\alpha \end{pmatrix},
 \end{aligned}$$

for $p \in \mathbf{R}^4$, $\alpha \in \{1, 2\}$ in which $\sigma = (\sigma_\mu)_{\mu=0}^3$, $\sigma_0 = 1_2$, $\{\sigma_i\}_{i=1}^3$ are the Pauli sigma matrices, $\{e_\alpha\}_{\alpha=1,2}$ is the standard basis for \mathbf{C}^2 and $q = p_1 - p_1'$ is the momentum transfer.

Lemma 1. *If the incoming and outgoing up quark momenta p_1 and p_1' are on shell and $\vec{p}_1 \neq \vec{0}$ then the momentum transfer $q = p_1 - p_1'$ is spacelike with*

$$q^2 < 0.$$

Proof We compute

$$\begin{aligned} q^2 &= (p_1 - p'_1)^2 = p_1^2 + p_1'^2 - 2p_1 \cdot p'_1 = 2(m_u^2 - p_1 \cdot p'_1) = 2(m_u^2 - p_1^0 p_1'^0 + \vec{p}_1 \cdot \vec{p}'_1) \\ &= 2(m_u^2 - \omega_{m_u}(\vec{p}_1) \omega_{m_u}(\vec{p}'_1) + \vec{p}_1 \cdot \vec{p}'_1) \\ &\leq 2(m_u^2 - \omega_{m_u}(\vec{p}_1) \omega_{m_u}(\vec{p}'_1) + |\vec{p}_1| |\vec{p}'_1|), \end{aligned}$$

where, for $m > 0$ and $\vec{p} \in \mathbf{R}^3$

$$\omega_m(\vec{p}) = (m^2 + |\vec{p}|^2)^{\frac{1}{2}}.$$

Consider the function $f : [0, \infty) \times [0, \infty)$ defined by

$$f(s, t) = m^2 + st - \omega_m(s) \omega_m(t), \text{ where } \omega_m(t) = (m^2 + t^2)^{\frac{1}{2}}.$$

Then $(\partial_2 f)(s, t) = s - \omega_m(s) \omega_m(t)^{-1} t$ (where ∂_2 means the partial derivative with respect to the second argument). Hence $(\partial_2 f)(s, t) = 0 \Leftrightarrow \omega_m(s)t = \omega_m(t)s \Leftrightarrow (m^2 + s^2)t^2 = (m^2 + t^2)s^2 \Leftrightarrow t = s$. Hence $t \mapsto f(s, t)$ is monotonic over $[0, s]$. Thus, since $f(s, 0) < 0$ for $s > 0$, $(\partial_2 f)(s, t) > 0 \Leftrightarrow s > t$ and $f(s, s) = 0$ it follows that $f(s, t) < 0, \forall t \in [0, s)$. But since $f(s, t) = f(t, s), \forall s, t > 0$ it follows that $f(s, t) < 0, \forall s, t > 0$. Therefore $q^2 < 0$ except when $\vec{p}_1 = \vec{p}'_1 = \vec{0}$. \square

From Eq. 30 we have that

$$\begin{aligned} \mathcal{M}_{i'_1 i'_2 \alpha'_1 \alpha'_2 i_1 i_2 \alpha_1 \alpha_2}^{(\text{tree})}(p'_1, p'_2, p_1, p_2) &= -\frac{g_s^2}{Q^2} \delta_{ab} \eta_{\mu\nu} T_{i'_1 i_1}^a T_{i'_2 i_2}^b \bar{u}(p'_1, \alpha'_1) \gamma^\mu u(p_1, \alpha_1) \bar{v}(p_2, \alpha_2) \gamma^\nu v(p'_2, \alpha'_2) \\ &= -\frac{g_s^2}{Q^2} \delta_{ab} \eta_{\mu\nu} T_{i'_1 i_1}^a T_{i'_2 i_2}^b \mathcal{M}_{0, i'_1 i'_2 \alpha'_1 \alpha'_2 i_1 i_2 \alpha_1 \alpha_2}^{\mu\nu}(p'_1, p'_2, p_1, p_2), \end{aligned} \tag{31}$$

where $Q = (-q^2)^{\frac{1}{2}}$ and

$$\mathcal{M}_{0, i'_1 i'_2 \alpha'_1 \alpha'_2 i_1 i_2 \alpha_1 \alpha_2}^{\mu\nu}(p'_1, p'_2, p_1, p_2) = \bar{u}(p'_1, \alpha'_1) \gamma^\mu u(p_1, \alpha_1) \bar{v}(p_2, \alpha_2) \gamma^\nu v(p'_2, \alpha'_2).$$

The vacuum polarization insertion is as shown in the Feynman diagram of Fig. 6 (this diagram stands for two diagrams, one with the quark bubble and the other with the gluon bubble). The Feynman amplitude associated with this

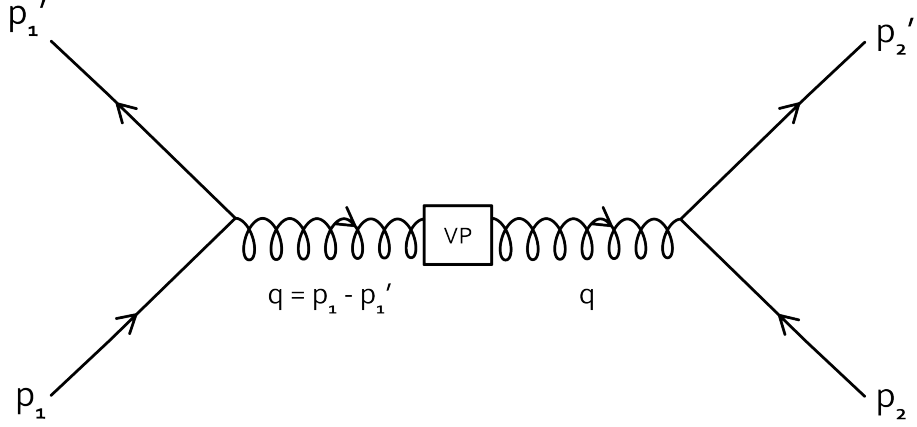


Figure 6: Vacuum polarization for quark $u\bar{d}$ scattering

diagram, $\mathcal{M}^{(\text{vp})}$, is given by

$$i\mathcal{M}_{i_1' i_2' \alpha_1' \alpha_2' i_1 i_2 \alpha_1 \alpha_2}^{(\text{vp})}(p_1', p_2', p_1, p_2) = \bar{u}(p_1', \alpha_1') i g_s T_{i_1' i_1}^a \gamma^\mu u(p_1, \alpha_1) \\ i D_{\text{QCD}, ac\mu\rho}(q) i \Pi^{(\text{vp}), cd\rho\sigma}(q) i D_{\text{QCD}, db\sigma\nu}(q) \\ \bar{v}(p_2, \alpha_2) i g_s T_{i_2 i_2'}^b \gamma^\nu v(p_2', \alpha_2'),$$

where D_{QCD} is the gluon propagator given by

$$D_{\text{QCD}, ab\mu\nu}(q) = -\frac{\delta_{ab}\eta_{\mu\nu}}{q^2 + i\epsilon},$$

and $\Pi^{(\text{vp})}$ is the total vacuum polarization tensor. Therefore

$$\mathcal{M}_{i_1' i_2' \alpha_1' \alpha_2' i_1 i_2 \alpha_1 \alpha_2}^{(\text{vp})}(p_1', p_2', p_1, p_2) = \frac{g_s^2}{Q^4} T_{i_1' i_1}^a T_{i_2 i_2'}^b \eta_{\mu\rho} \eta_{\sigma\nu} \delta_{ac} \delta_{db} \Pi^{(\text{vp}), cd\rho\sigma}(q) \\ \mathcal{M}_{0, i_1' i_2' \alpha_1' \alpha_2' i_1 i_2, \alpha_1 \alpha_2}^{\mu\nu}(p_1', p_2', p_1, p_2).$$

Now

$$\Pi^{(\text{vp})} = \Pi^{(q)} + \Pi^{(g)} + \Pi^{(4)},$$

and from the previous section $\Pi^{(4)} = 0$,

$$\Pi^{(q)ab\mu\nu}(q) = \frac{1}{3\pi} g_s^2 \delta^{ab} \sum_{k=1}^6 f(m_k, Q) (Q^2 \eta^{\mu\nu} - q^\mu q^\nu),$$

and

$$\Pi^{(g)ab\mu\nu}(q) = -\frac{19}{32\pi}g_s^2\delta^{ab}\eta^{\mu\nu}Q^2 - \frac{3}{32\pi^2}g_s^2\delta^{ab}q^\mu q^\nu Q^{-1}\sigma_2^{(g)}(Q). \quad (32)$$

where

$$f(m, Q) = m^3Q^{-3}Z(m, Q)(3 + 2Z(m, Q)^2),$$

and $Q = (-q^2)^{\frac{1}{2}}$.

By a well known conservation property (Weinberg, 2005, [27], p. 480), we can, in the presence of the factor $\mathcal{M}_0^{\mu\nu}$, drop the terms involving $q^\mu q^\nu$. Therefore

$$\begin{aligned} & \mathcal{M}_{i'_1 i'_2 \alpha'_1 \alpha'_2 i_1 i_2 \alpha_1 \alpha_2}^{(\text{vp})}(p'_1, p'_2, p_1, p_2) \\ &= \frac{g_s^2}{Q^2} T_{i'_1 i_1}^a T_{i'_2 i_2}^b \eta_{\mu\rho} \eta_{\sigma\nu} \delta_{ac} \delta_{db} \\ & \quad \left(\frac{1}{3\pi} g_s^2 \delta^{cd} \eta^{\rho\sigma} \sum_{k=1}^6 f(m_k, Q) - \frac{19}{32\pi} g_s^2 \delta^{cd} \eta^{\rho\sigma} \right) \\ & \quad \mathcal{M}_{0, i'_1 i'_2 \alpha'_1 \alpha'_2 i_1 i_2 \alpha_1 \alpha_2}^{\mu\nu}(p'_1, p'_2, p_1, p_2) \\ &= -\frac{g_s^2}{Q^2} T_{i'_1 i_1}^a T_{i'_2 i_2}^a \mathcal{M}_{0, i'_1 i'_2 \alpha'_1 \alpha'_2 i_1 i_2 \alpha_1 \alpha_2}(p'_1, p'_2, p_1, p_2) \pi^{(s)}(Q), \end{aligned}$$

where

$$\pi^{(s)}(Q) = g_s^2 \left(\frac{19}{32\pi} - \frac{1}{3\pi} \sum_{k=1}^6 f(m_k, Q) \right),$$

and

$$\mathcal{M}_0 = \eta_{\mu\nu} \mathcal{M}_0^{\mu\nu}.$$

The total Feynman amplitude $\mathcal{M} = \mathcal{M}^{(\text{tree})} + \mathcal{M}^{(\text{vp})}$ is given by

$$\begin{aligned} & \mathcal{M}_{i'_1 i'_2 \alpha'_1 \alpha'_2 i_1 i_2 \alpha_1 \alpha_2}(p'_1, p'_2, p_1, p_2) \\ &= -\frac{g_s^2}{Q^2} T_{i'_1 i_1}^a T_{i'_2 i_2}^a \mathcal{M}_{0, i'_1 i'_2 \alpha'_1 \alpha'_2 i_1 i_2 \alpha_1 \alpha_2}(p'_1, p'_2, p_1, p_2) (1 + \pi^{(s)}(Q)). \end{aligned}$$

4.2 Computation of the quantity $\Gamma = \Gamma(q)$ such that $\mathcal{M} = \Gamma \mathcal{M}^{(\text{tree})}$

Consider the quantity $\Gamma : \{q \in \mathbf{R}^4 : q^2 < 0\} \rightarrow \mathbf{C}$, a function of the momentum transfer q which, if it exists, specifies over all values of the input and output momenta and polarizations, a relationship of proportionality between the total Feynman amplitude \mathcal{M} and the tree amplitude $\mathcal{M}^{(\text{tree})}$. Γ is given by the

following equation (if the solution of the equation exists)

$$\mathcal{M} = \Gamma(q)\mathcal{M}^{(\text{tree})}.$$

This is equivalent to the following

$$\begin{aligned} & -\frac{g_s^2}{Q^2}T_{i'_1 i_1}^a T_{i'_2 i_2}^a \mathcal{M}_{0,i'_1 i'_2 \alpha'_1 \alpha'_2 i_1 i_2 \alpha_1 \alpha_2}(p'_1, p'_2, p_1, p_2)(1 + \pi^{(s)}(Q)) \\ & = -\Gamma(q)\frac{g_s^2}{Q^2}T_{i'_1 i_1}^a T_{i'_2 i_2}^a \mathcal{M}_{0,i'_1 i'_2 \alpha'_1 \alpha'_2 i_1 i_2 \alpha_1 \alpha_2}(p'_1, p'_2, p_1, p_2), \end{aligned} \quad (33)$$

for all sets of momenta and polarizations. This equation has the unique solution

$$\Gamma(q) = 1 + \pi^{(s)}(Q) = 1 + g_s^2\left(\frac{19}{32\pi} - \frac{1}{3\pi} \sum_{k=1}^6 f(m_k, Q)\right), \quad (34)$$

for $Q = (-q^2)^{\frac{1}{2}}$ and we see that Γ exists and is real valued. We can write, without fear of confusion,

$$\Gamma(Q) = \Gamma(g_s, Q) = 1 + g_s^2\left(\frac{19}{32\pi} - \frac{1}{3\pi} \sum_{k=1}^6 f(m_k, Q)\right), \quad (35)$$

for $Q > 0$.

4.3 Computation of the momentum space QCD coupling $q \mapsto g_s(q)$

From Eq. 31 we may write that the momentum space QCD coupling $q \mapsto g_s(q)$ as a function of momentum transfer q is given by

$$\mathcal{M}_{i'_1 i'_2 \alpha'_1 \alpha'_2 i_1 i_2 \alpha_1 \alpha_2}(p'_1, p'_2, p_1, p_2) = -\frac{g_s(q)^2}{Q^2}T_{i'_1 i_1}^a T_{i'_2 i_2}^a \mathcal{M}_{0,i'_1 i'_2 \alpha'_1 \alpha'_2 i_1 i_2 \alpha_1 \alpha_2}(p'_1, p'_2, p_1, p_2), \quad (36)$$

that is if, indeed, there exists a function $q \mapsto g_s(q)$ of momentum transfer such that the total Feynman amplitude \mathcal{M} can be written in this form. But we have

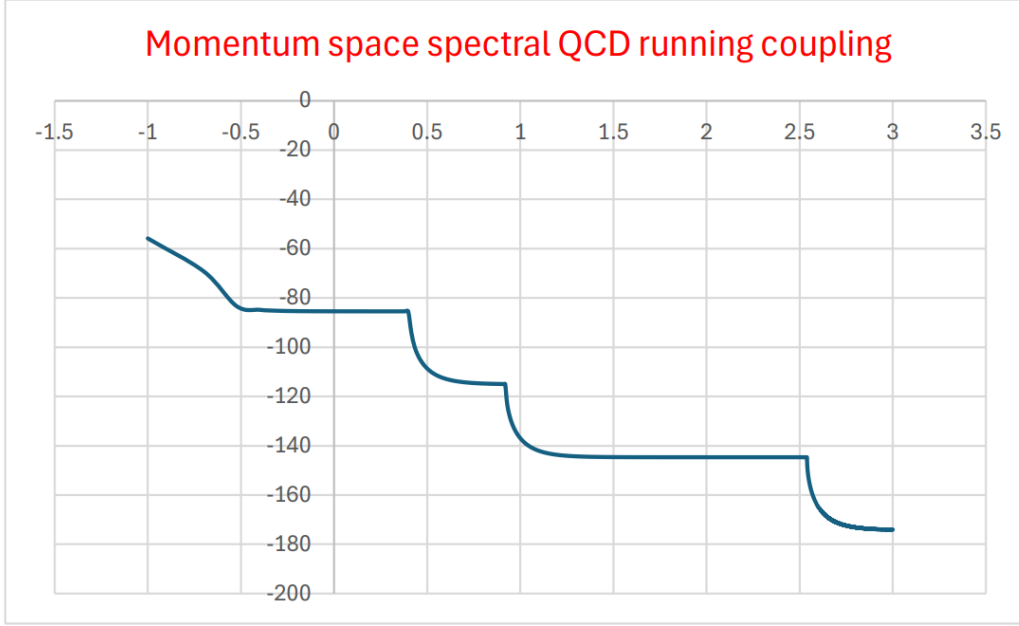


Figure 7: Untransformed momentum space spectral QCD running coupling vs. log of energy in GeV

just shown that

$$\begin{aligned}
 \mathcal{M}_{i'_1 i'_2 \alpha'_1 \alpha'_2 i_1 i_2 \alpha_1 \alpha_2}(p'_1, p'_2, p_1, p_2) &= \Gamma(q) \mathcal{M}_{i'_1 i'_2 \alpha'_1 \alpha'_2 i_1 i_2 \alpha_1 \alpha_2}^{(\text{tree})}(p'_1, p'_2, p_1, p_2) \\
 &= -\Gamma(q) \frac{g_s^2}{Q^2} T_{i'_1 i_1}^a T_{i'_2 i_2}^a \mathcal{M}_{0, i'_1 i'_2 \alpha'_1 \alpha'_2 i_1 i_2 \alpha_1 \alpha_2}(p'_1, p'_2, p_1, p_2).
 \end{aligned} \tag{37}$$

Therefore we may equate the right hand sides of Eqns. 36 and 37 and make cancellations to show that the (one-loop) momentum space QCD coupling $q \mapsto g(q)$ is given by

$$g(q)^2 = g_s^2 \Gamma(q) \text{ and } g(Q)^2 = g_s^2 \Gamma(Q).$$

We denote the constant g_s by g_b and call it the bare coupling constant. In our work g_b is finite. Γ depends (implicitly) on g_b (see Eq. 34). $\alpha(Q) = \frac{g(Q)^2}{4\pi} = \frac{g_b^2}{4\pi} \Gamma(Q) = \alpha_b \Gamma(Q)$ is the energy space running QCD fine structure constant, where $\alpha_b = \frac{g_b^2}{4\pi}$ is the bare QCD fine structure constant.

The graph of the momentum space spectral QCD running coupling (with $\alpha_b = 1$) is shown in Fig. 7.

5 The position space spectral QCD running coupling

The function $\Gamma : \{q \in \mathbf{R}^4 : q^2 < 0\}$ defined by Eq. 34 gives (after multiplication by α_b) the untransformed momentum space QCD coupling. The position space QCD coupling is given, formally, by taking the inverse Fourier transform of $q \mapsto \Gamma(q)$ according to

$$\Gamma(x) = (2\pi)^{-4} \int \Gamma(q) e^{iq \cdot x} dq \text{ for } x \in \mathbf{R}^4.$$

The position space QCD running coupling as a function of distance $r > 0$ is given, formally, by

$$\Gamma(r) = (2\pi)^{-4} \int \Gamma(q) e^{iq \cdot (0,0,0,r)} dq. \quad (38)$$

$q \mapsto \Gamma(q)$ is not an L^1 function or an L^2 function and it is straightforward to show that the integral given by Eq. 38 is not convergent.

Therefore we introduce a momentum-energy cutoff $\Lambda > 0$ and write, using spherical polar coordinates for \vec{q} where $q = (q^0, \vec{q})$,

$$\begin{aligned} \Gamma_\Lambda(r) &= (2\pi)^{-4} \int_{S_\Lambda} \Gamma(q) e^{iq \cdot (0,0,0,r)} dq \\ &= (2)(2\pi)^{-4} (2\pi) \int_{\rho=0}^\Lambda \int_{E=0}^\rho \int_{\theta=0}^\pi \Gamma((\rho^2 - E^2)^{\frac{1}{2}}) e^{-i\rho \cos(\theta)r} \rho^2 \sin(\theta) d\theta dE d\rho \\ &= \frac{1}{4\pi^3} \int_{\rho=0}^\Lambda \int_{E=0}^\rho \Gamma((\rho^2 - E^2)^{\frac{1}{2}}) \frac{1}{i\rho r} e^{i\rho r u} \Big|_{u=-1}^1 \rho^2 dE d\rho \\ &= \frac{1}{2\pi^3} \frac{1}{r} \int_{\rho=0}^\Lambda \int_{E=0}^\rho \Gamma((\rho^2 - E^2)^{\frac{1}{2}}) \rho \sin(\rho r) dE d\rho, \end{aligned}$$

where $S_\Lambda = \{q \in \mathbf{R}^4 : -\Lambda^2 < q^2 < 0, |q^0| < |\vec{q}|\}$.

Therefore the (cut off) QCD running coupling $\tau \mapsto \Gamma_\Lambda(\tau)$ as a function of (collision) energy τ is given by

$$\Gamma_\Lambda(\tau) = \frac{1}{2\pi^3} \tau \int_{\rho=0}^\Lambda \int_{E=0}^\rho \Gamma((\rho^2 - E^2)^{\frac{1}{2}}) \rho \sin(\rho/\tau) dE d\rho.$$

Letting $\xi = (\rho^2 - E^2)^{\frac{1}{2}}$ we have $\xi^2 = \rho^2 - E^2$ so, for any fixed ρ , $dE = -d\xi$

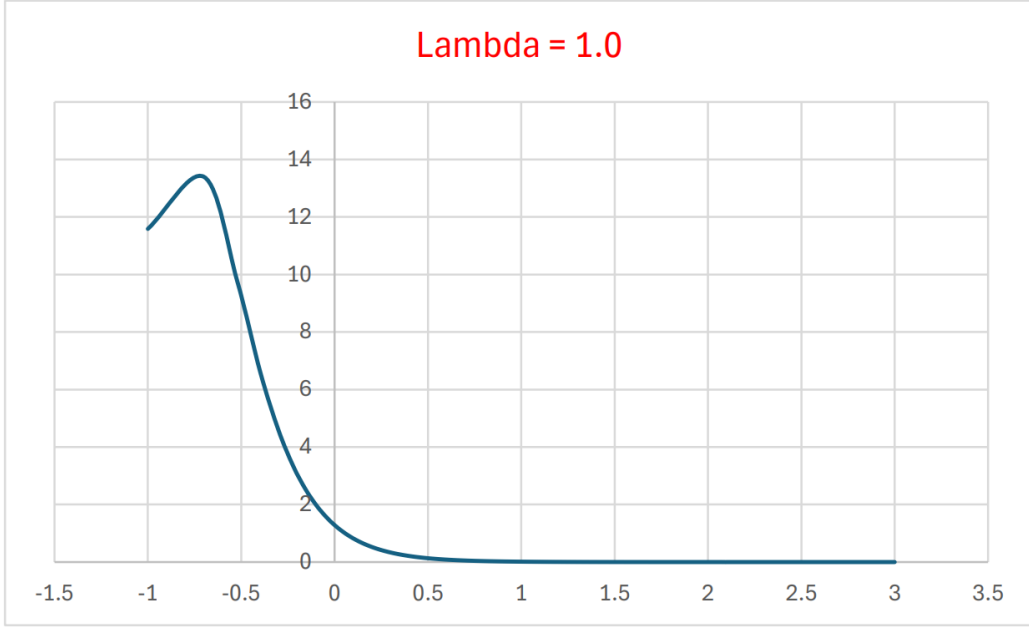


Figure 8: Shifted Γ_Λ vs. log of energy in GeV for $\Lambda = 1.0$ GeV

from which it follows that

$$\Gamma_\Lambda(\tau) = \frac{1}{2\pi^3} \tau \int_{\rho=0}^{\Lambda} \left(\int_{\xi=0}^{\rho} \Gamma(\xi) d\xi \right) \rho \sin(\rho/\tau) d\rho.$$

(No confusion need arise through using the same symbol for Γ in all its guises, i.e. a momentum space function $q \mapsto \Gamma(q)$, a position space function $x \mapsto \Gamma(x)$, a function of distance r and a function of energy τ .)

Graphs of (the absolute value of) this function for various values of the cutoff energy Λ (and $\alpha_b = 1$) are shown in Figs. 8, 9 and 10. We have translated each of these graphs along the y-axis (i.e. the α axis) so that their limiting value is zero as $\tau \rightarrow \infty$ (the explanation and justification for this will be given in the next section).

As Λ is increased the running coupling graph shifts to the right and the α values are scaled up while if Λ is decreased the graph moves to the left and the α values are scaled down. In all cases the running coupling manifests asymptotic freedom and, while not having a Landau pole, has what might be described as a “Landau peak” together with subsidiary subpeaks.

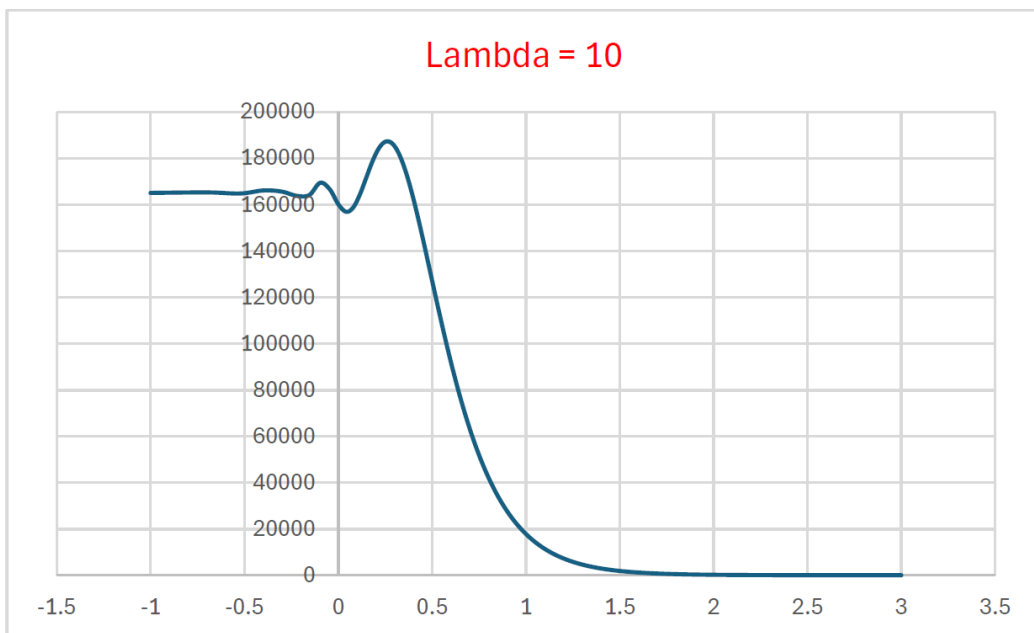


Figure 9: Shifted Λ_Γ vs. log of energy in GeV for $\Lambda = 10$ GeV

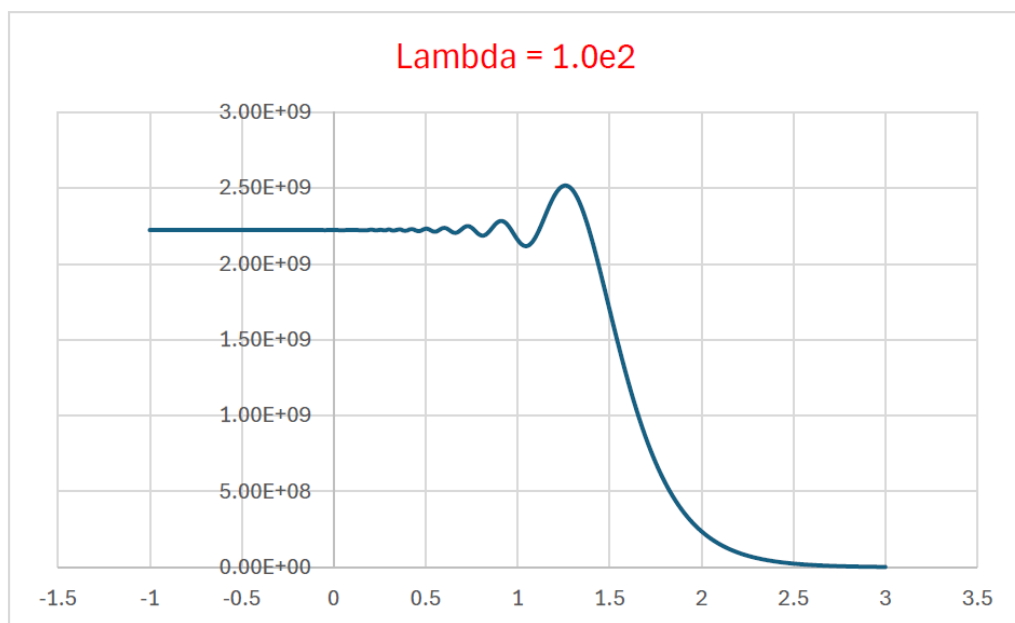


Figure 10: Shifted Γ_Λ vs. log of energy in GeV for $\Lambda = 100$ GeV

6 Comparison of the spectral QCD running coupling with CERN data

The QCD coupling is not an observable and, when its computation involves renormalization, it is renormalization scheme (RS) dependent. The RS affects the unrenormalized regularized vacuum polarization function by the addition of a constant. For example, with Pauli-Villars regularization the unrenormalized quark bubble vacuum polarization function is given by (Itzykson and Zuber, 1980 [28], p. 323)

$$\pi(k^2, m, \Lambda) = -\frac{\alpha}{3\pi} \left\{ -\log\left(\frac{\Lambda^2}{m^2}\right) + \frac{1}{3} + 2 \left(1 + \frac{2m^2}{k^2}\right) \left[\left(\frac{4m^2}{k^2} - 1\right)^{\frac{1}{2}} \right. \right. \\ \left. \left. \times \operatorname{arccot} \left(\frac{4m^2}{k^2} - 1 \right)^{\frac{1}{2}} - 1 \right] \right\},$$

where Λ is the fictitious mass parameter and therefore the counterterm is $\frac{\alpha}{3\pi} \log(\frac{\Lambda^2}{m^2})$. For dimensional regularization the unrenormalized quark bubble vacuum polarization function is given by (Schwartz, 2018 [24], p. 309)

$$\pi(p^2) = -\frac{g_s^2}{2\pi^2} \int_0^1 dx x(1-x) \left[\frac{2}{\epsilon} + \log \left(\frac{(4\pi e^{-\gamma_E} \mu)^2}{m^2 - p^2 x(1-x)} \right) \right], \quad (39)$$

where μ is the subtraction point. For MS RS scheme the counterterm involves the factor $\frac{1}{\epsilon}$ while for $\overline{\text{MS}}$ RS scheme the counterterm involves the factor $\frac{1}{\epsilon} + \log(4\pi e^{-\gamma_E})$. In fact, for the so called \mathcal{R}_δ RS [29] an arbitrary value δ is added. In any case the effect of a change in RS is the addition of a constant to the counterterm.

Spectral regularization is finite at all stages and no renormalization is required, there are no counterterms.

To compare our predictions with data which has been obtained from experimental data using calculations based on the $\overline{\text{MS}}$ RS we need to add a suitable constant to our running coupling function. If all the calculations of the running fine structure constant at any given energy based on experiments were done using covariant spectral regularization then no such constant would be required.

Therefore, for the purpose of comparing our spectral running coupling with the $\overline{\text{MS}}$ running coupling or running coupling data interpreted through $\overline{\text{MS}}$ we

can write that the spectral running coupling at energy τ is

$$\Gamma_{\Lambda}(\tau) = \alpha_b \Gamma_{\Lambda,0}(\tau) + c, \quad (40)$$

for some $c \in \mathbf{R}$ and $\alpha_b > 0$, where

$$\Gamma_{\Lambda,0}(\tau) = \frac{1}{2\pi^3} \tau \int_{\rho=0}^{\Lambda} \left(\int_{\xi=0}^{\rho} \Gamma(\xi) d\xi \right) \rho \sin(\rho/\tau) d\rho.$$

Since Γ depends (implicitly) on α_b we should write $\Gamma_{\Lambda,0} = \Gamma_{\Lambda,0}(\alpha_b, \tau)$.

To find the values of α_b and c which give the best (in a certain sense) correspondence between Γ_{Λ} and a collection $\{(\tau_i, \alpha_i) : i = 1, \dots, n\}$ of running coupling data, such as the CERN data, we note that any function of the form

$$\Gamma_{\Lambda}(\alpha_b, \tau) = \alpha_n + \frac{\alpha_1 - \alpha_n}{\Gamma_{\Lambda,0}(\alpha_b, \tau_1) - \Gamma_{\Lambda,0}(\alpha_b, \tau_n)} (\Gamma_{\Lambda,0}(\alpha_b, \tau) - \Gamma_{\Lambda,0}(\alpha_b, \tau_n)), \quad (41)$$

passes through the points (τ_1, α_1) and (τ_n, α_n) . Thus we have scaled $\Gamma_{\Lambda,0}$ and translated it along the y-axis (i.e. the α axis) so that the graph of the function Γ_{Λ} passes through the points (τ_1, α_1) and (τ_n, α_n) . Eq. 41 is invariant under the transformation

$$\Gamma_{\Lambda,0} \mapsto \lambda \Gamma_{\Lambda,0},$$

for any $\lambda \in \{-1, 1\}$ (or, more generally, $\lambda \in \mathbf{R}, \lambda \neq 0$). (This is a specific example of the fact that the physics of a process is determined by $|\mathcal{M}|$ where \mathcal{M} is its Feynman amplitude (more generally, by rays in Hilbert space of Feynman amplitudes for the process.)) Thus we may take the spectral running coupling at energy τ to be

$$\Gamma_{\Lambda}(\alpha_b, \tau) = -\alpha_b \Gamma_{\Lambda,0}(\alpha_b, \tau) + c, \quad (42)$$

for some $c \in \mathbf{R}, \alpha_b > 0$.

Therefore, from Eqns. 41 and 42 we seek $\alpha_b, c \in \mathbf{R}$, with $\alpha_b > 0$ such that

$$\alpha_b = -(\alpha_1 - \alpha_n) (\Gamma_{\Lambda,0}(\alpha_b, \tau_1) - \Gamma_{\Lambda,0}(\alpha_b, \tau_n))^{-1}, \quad (43)$$

and

$$c = \alpha_n + \alpha_b \Gamma_{\Lambda,0}(\alpha_b, \tau_n). \quad (44)$$

Analytical solution of this problem would require solution of a complicated integral equation, that is Eq. 43, to determine α_b , and then the plugging in of the solution to that equation into Eq. 44 to determine c . Fortunately the problem given by Eq. 43 can be solved computationally using the following

(fixed point computation) algorithm.

Algorithm 1. Carry out the following computation to determine the bare spectral QCD fine structure constant α_b .

1. initialize $\alpha_b = 1$
2. compute $d = -(\alpha_1 - \alpha_n)(\Gamma_{\Lambda,0}(\alpha_b, \tau_1) - \Gamma_{\Lambda,0}(\alpha_b, \tau_n))^{-1}$
3. compute $\Delta = d - \alpha_b$
4. set $\alpha_b = d$
5. repeat steps 2, 3, and 4 until Δ vanishes

We have found that this algorithm converges in less than 20 iterations. The value to which it converges, i.e. the QCD bare fine structure constant, depends on the cutoff Λ . The optimum value of Λ where the running coupling agrees best with CERN experimental data occurs when Λ is about 14 GeV. For this value of Λ the Landau peak occurs at about a few hundred MeV and the bare QCD fine structure constant has the value $\alpha_b = 0.00219608$.

Thus it seems that we can conclude, since $\alpha_b \ll 1$, that, when analyzed using spectral regularization, QCD is perturbative at all energies, i.e. perturbation theory can be successfully used, at all energies.

The distance corresponding to an energy of 14 GeV is given by

$$d = \left(\frac{hc}{e}\right)\left(\frac{1}{14 \times 10^9 eV}\right) \approx 8.86 \times 10^{-17} m,$$

(where h is Planck's constant, c is the speed of light and e is the charge of the electron) which is about of the order of the radius of a meson or baryon. The graph of the QCD running coupling versus energy (inverse distance) when $\Lambda = 14$ GeV is shown in Fig. 11.

Using the values for α_b obtained by using Algorithm 1 and then the value of c obtained by using Eq. 44 the one-loop QCD running coupling versus CERN $\overline{\text{MS}}$ data is shown in Fig. 12.

Our spectral running coupling has the same general shape as the $\overline{\text{MS}}$ CERN data curve over the range of the CERN data but it does not agree exactly. However the CERN data curve is RS dependent, use of another RS, other than $\overline{\text{MS}}$, in analyzing the experimental data would result in a different CERN data curve. Fig. 13 shows the QCD running coupling computed using renormalization for a number of different renormalization schemes and/or IR completions. It can be seen that there is a range of possible QCD running coupling curves.

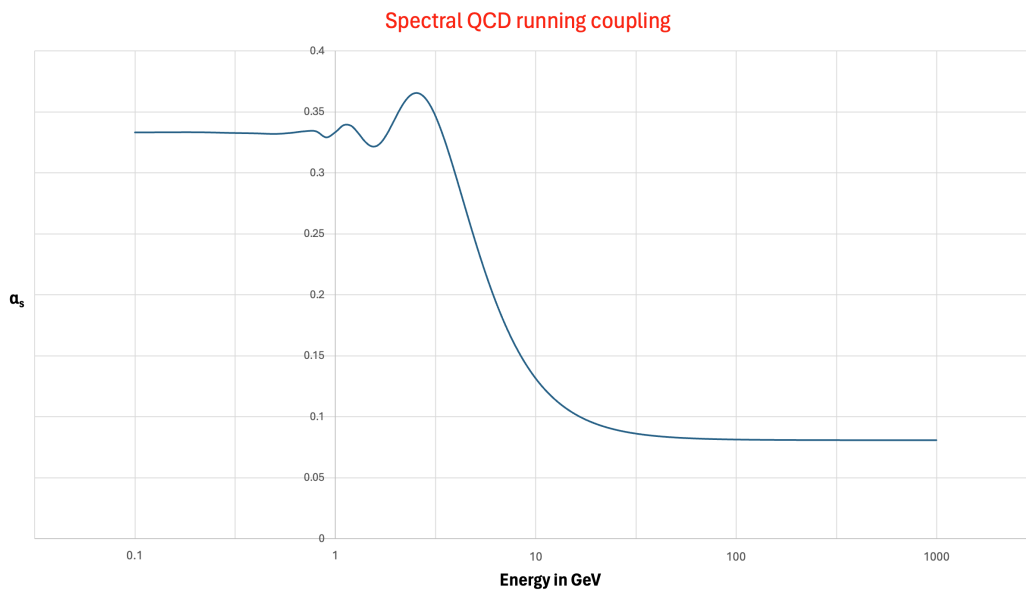


Figure 11: Spectral QCD running coupling versus energy in GeV

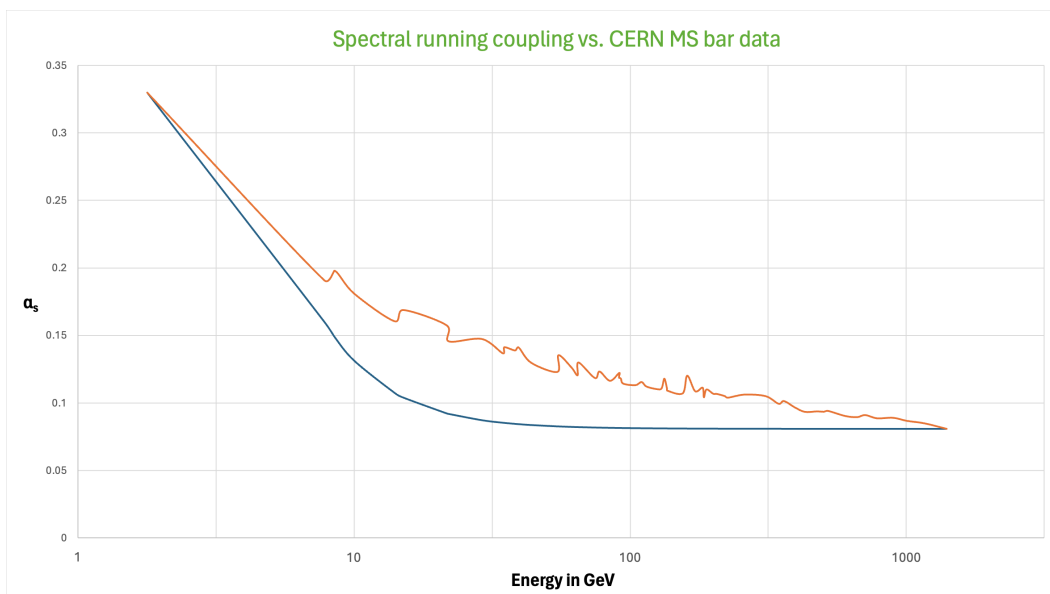


Figure 12: Spectral QCD running coupling versus CERN \overline{MS} data. Data courtesy of CERN

Spectral regularization provides a method for computing the QCD running coupling which is distinct from that associated with the $\overline{\text{MS}}$ RS and also to all other possible RSs for the renormalization method.

We propose that if covariant spectral regularization were used to analyze the CERN experimental data to produce the CERN data curve, then the CERN data curve would coincide with our theoretically computed spectral QCD running coupling curve.

7 Freezing of $\alpha_s(\tau)$ as energy $\tau \rightarrow 0$

At low energies the running coupling computed using renormalization in the UV together with other standard approaches (such as α_T, α_{g_1} , or $\hat{\alpha}_{\text{PI}}$) for IR completion has the property of “freezing” in the IR. The freezing behavior is RS and IR completion scheme dependent. The nature of this dependence is illustrated in Fig. 14.

The spectral QCD running coupling also manifests the property of freezing at low energies as can be seen by examination of Fig. 11. Thus, one says that spectral running coupling saturates in the IR, i.e. has an IR fixed point.

The spectral QCD running coupling does not manifest an unphysical Landau pole. It has this property in common with the spectral QED running coupling which we have shown [21] also does not manifest a Landau pole. However the spectral QCD running coupling manifests what may be called a “Landau peak” at an energy of a few hundred MeV, together with subsidiary subpeaks (see Fig. 11).

8 Conclusion

This paper focuses on spectral QCD vacuum polarization in order to compute the spectral QCD running coupling by comparing $\mathcal{M}^{(\text{tree})}$ with $\mathcal{M} = \mathcal{M}^{(\text{tree})} + \mathcal{M}^{(\text{vp})}$ for quark $u\bar{d} \rightarrow u\bar{d}$ scattering. Using covariant spectral regularization we compute the densities associated with the quark bubble and the gluon bubble and hence the spectral vacuum polarization tensor. We then compute and display the spectral QCD running coupling.

The spectral QCD running coupling is not constructed by piecing together or matching functions defined in the perturbative and non-perturbative domains, by Padé approximant or other means, but is defined by a single exact, well defined unified prescription over the whole CM energy range, both perbutave

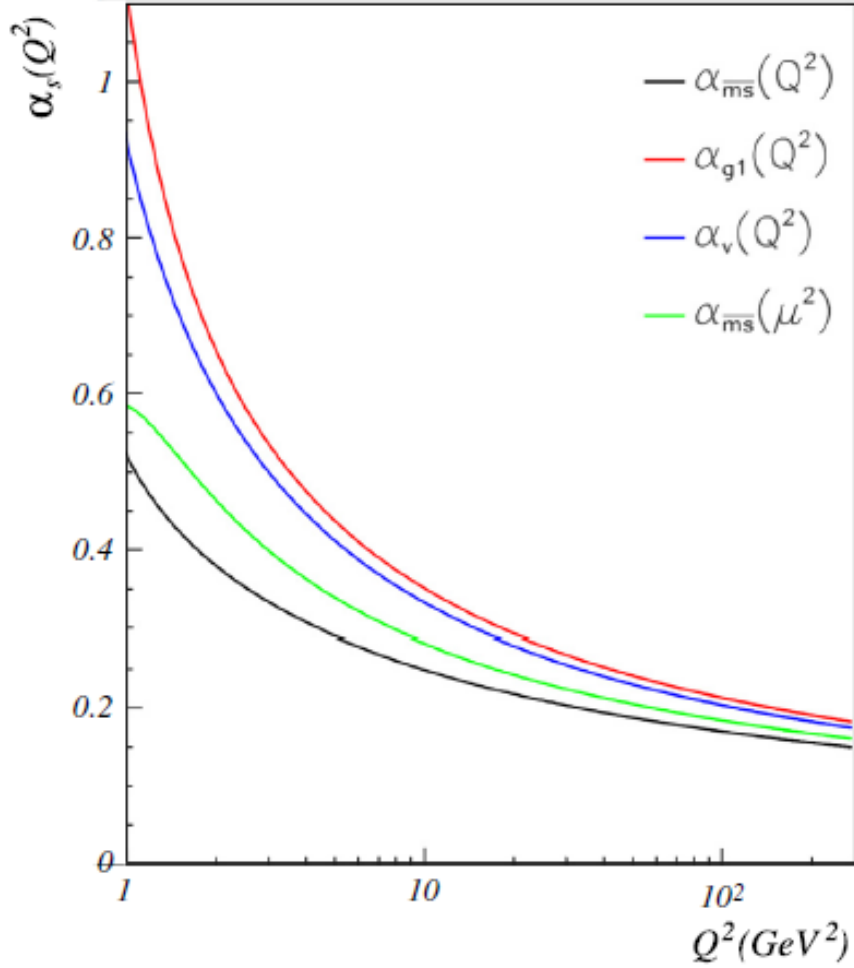


Figure 13: The strong coupling $\alpha_s(Q^2)$ expressed in different renormalization schemes (black: $\overline{\text{MS}}$ -scheme, red: g_1 effective charge, blue: V-scheme) and using a scale $\mu \neq Q$ (green). We chose $\mu = 0.708 Q$ which, in the CSR context, is the LO scale shift transforming $\alpha_{\overline{\text{MS}}}$ into α_R (α_R is the effective charge obtained from the ratio of the $e^+ + e^- \rightarrow \text{hadrons}$ to that for $e^+ + e^- \rightarrow \mu^+ + \mu^-$). In this figure $\overline{\text{MS}}$ was computed with $n_f = 3$, $\Lambda = 0.34 \text{ GeV}$ and to order β_2 . (For interpretation of the references to colour in this figure legend, the reader is referred to the web version of the article.)

Source Deur et al., 2016 [8], Fig. 3.4

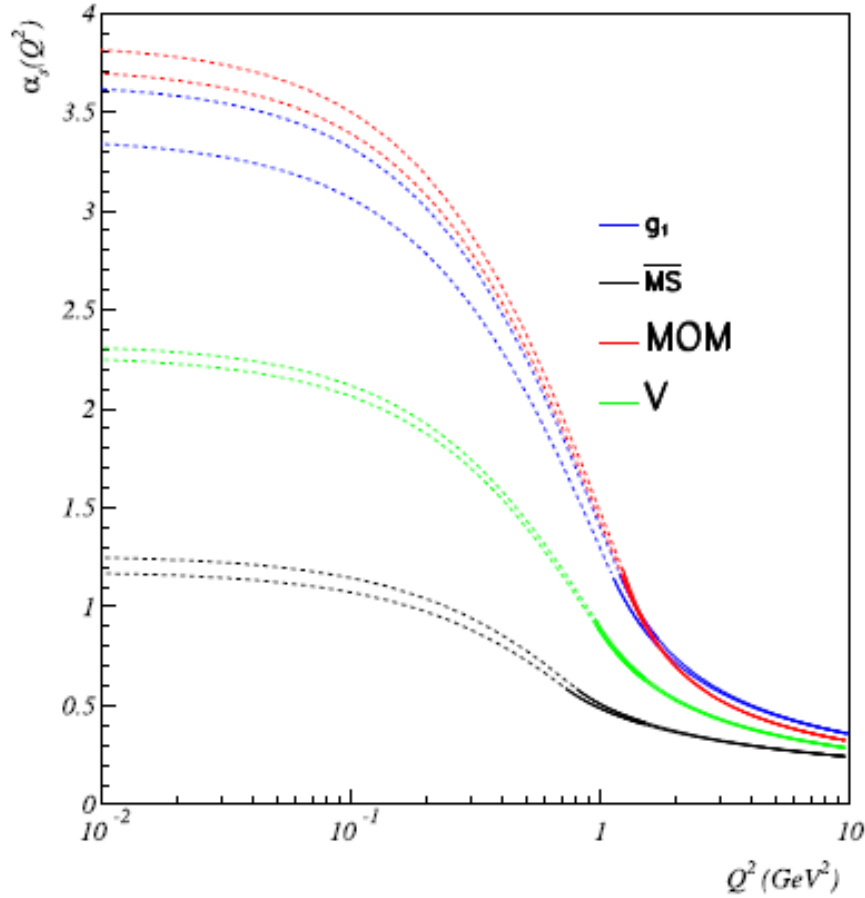


Figure 14: How different renormalization schemes lead to different freezing values for α_s . The black dashed line represents the AdS/QCD continuation of α_{pQCD} in the $\overline{\text{MS}}$ scheme (continuous black line), the blue line is the effective charge α_{g_1} in the g_1 scheme (without enforcing the $\alpha_{g_1}(0) = \pi$ constraint), the green line is the effective charge α_V in the potential scheme and the red line is α_s in the MOM scheme and Landau gauge. The widths of the curves represent the uncertainty stemming from the truncation of the pQCD β -series. For interpretation of the references to colour in this figure legend the reader is referred to the web version of this article.) **Source:** Deur et al., 2016 [8], Fig. 5.1

and non-perturbative. In fact we have shown that, when analyzed using spectral regularization, it seems that QCD is perturbative at all energies.

It is a purely theoretical construct, not requiring any input data derived from experiment or lattice simulation other than the quark masses. Apart from the quark masses the only parameter which needs to be input in order to generate the running coupling function is the energy cutoff. This energy cutoff seems to be related to the typical hadron size.

The spectral running coupling is an analytic function which does not manifest an unphysical Landau pole but rather, what may be called a “Landau peak” (together with subsidiary subpeaks). It has the property of freezing in the infrared.

The spectral QCD running coupling has the desirable properties of interoperability, simplicity and finiteness mentioned at the end of the article (Deur 2016, [8]).

Acknowledgements

The author thanks Günther Dissertori and Siegfried Bethke for providing, and allowing the use of, the CERN QCD running coupling data obtained from LHC hadron collider experiments, lattice simulations, Z^0 pole fit, e^+e^- annihilation and other sources, published in the 2018 Particle Data Group Review of Particle Physics [30]. Also the author thanks Alexandre Deur for helpful correspondence and allowing the use of two figures from his 2016 paper [8].

References

- [1] d’Enterria, D., Kluth, S. and Zanderighi, G., The strong coupling constant: State of the art and the decade ahead (Snowmass 2021 White Paper) (2021)
- [2] Dissertori, G., Knowles, I. and Schmelling, M., Quantum Chromodynamics, Oxford University Press, Cambridge U.K. (2003)
- [3] Hinchliffe, I. and Manohar, A., The QCD Coupling Constant, Annual Review of Nuclear and Particle Science 50, 643-678 (2000)
- [4] Prosperi, G. M., Raciti, M. and Simolo, C., On the running coupling constant in QCD, Progress in Particle and Nuclear Physics 58, 387–438 (2007)

- [5] Ducloué, B., Iancu, E., Lappi, T., Mueller, A. H., Soyez, G., Triantafyllopoulos, D. N. and Zhu, Y., Use of a running coupling in the NLO calculation of forward hadron production, *Physical Review D* 97, 054020 (2018)
- [6] Aoki *et al*, Y., FLAG Review 2021 (Flavour Lattice Averaging Group (FLAG)), *European Physics Journal* 82:869 (2022)
- [7] Deur, A., Brodsky, S. J. and Roberts, C. D., QCD running couplings and effective charges, *Progress in Particle and Nuclear Physics* 134, 104081 (2024)
- [8] Deur, A., Brodsky, S. J. and Teramond, G. F., The QCD running coupling, *Progress in Particle and Nuclear Physics* 90, 1-74 (2016)
- [9] Gross, D. J. and Wilczek, F., Ultraviolet Behavior of Non-Abelian Gauge Theories, *Physical Review Letters* 30(26), 1343-1346 (1973)
- [10] Politzer, H. D., Reliable Perturbative Results for Strong Interactions?, *Physical Review Letters* 30(26), 1346-1349 (1973)
- [11] Wu, X.-G., Brodsky, S. J. and Mojaza, M., The renormalization scale-setting problem in QCD, *Progress in Particle and Nuclear Physics* 72 44–98 (2013)
- [12] Wu, X.-G., Wang, S.-Q. and Brodsky, S. J., Importance of proper renormalization scale-setting for QCD testing at colliders, *Frontiers in Physics* 11(1), 111201 (2016)
- [13] Brodsky, S. J., Lepage, G. P. and Mackenzie, P. B., On the elimination of scale ambiguities in perturbative quantum chromodynamics, *Physical Review D* 28, 228 (1983)
- [14] Gell-Mann, M. and Lo, F. E., Quantum electrodynamics at small distances, *Physical Review* 95(5), 1300-1312 (1954)
- [15] Callan, C. G. (Jr.), Broken scale invariance in scalar field theory, *Physical Review D* 2(8), 1541-1547 (1970)
- [16] Symanzik, K., Small distance behaviour in field theory and power counting, *Communications in Mathematical Physics* 18, 227-246 (1970)
- [17] Binosi, D., Mezrag, C., Pappavassiliou, J., Roberts, C. D. and Rodríguez-Quintero, J., Process-independent strong running coupling, *Physical Review D* 96, 054026 (2017)
- [18] Mashford, J., An introduction to spectral regularization for quantum field theory, in *Proceedings of XIII International Workshop on Lie Theory and*

- Its Applications in Physics (Varna, Bulgaria, June 2019), Springer Proceedings in Mathematics and Statistics, Vol. 335, ed. V. Dobrev, Springer, Heidelberg-Tokyo (2020)
- [19] Mashford, J., A Spectral Calculus for Lorentz Invariant Measures on Minkowski Space, *Symmetry*, 12(10), 1696 (2020)
 - [20] Mashford, J., Divergence-free quantum electrodynamics in locally conformally flat space-time, *International Journal of Modern Physics A*, 36(13), 2150083 (2021)
 - [21] Mashford, J., Spectral regularization and a QED running coupling without a Landau pole, *Nuclear Physics B*, Volume 969, 115467 (2021)
 - [22] Mashford, J., UV and IR divergence-free calculation of the vertex function at arbitrary values of its arguments, arXiv:2203.07903 (2022)
 - [23] Peskin, M. E. and Schroeder, D. V., *Quantum Field Theory*, Westview Press (1995)
 - [24] Schwartz, M. D., *Quantum Field Theory and the Standard Model*, Cambridge University Press, Cambridge U.K. (2018)
 - [25] Mashford, J., Computation of the masses of the elementary particles, *AIP Advances* 14, 015007 (2024)
 - [26] Mashford, J., Computation of the leading order contributions to the Lamb shift for the H atom using spectral regularization, arXiv:2009.07644 (2020)
 - [27] Weinberg, S., *The Quantum Theory of Fields*, Cambridge University Press, Cambridge, U.K. (2015)
 - [28] Itzykson, C. and Zuber, B., *Quantum Field Theory*, McGraw-Hill, New York (1980)
 - [29] Mojaza, M., Brodsky, S. J. and Wu, X.-G., Systematic all-orders method to eliminate renormalization-scale and scheme ambiguities in perturbative QCD, *Physical Review Letters* 110, 192001 (2013)
 - [30] Tanabashi, M. et al. (Particle Data Group), Review of Particle Physics, *Physical Review D* 98, 030001 (2018)

Appendix: C++ code used to generate graphs in paper

```

#include "pch.h"
#include <iostream>
#include <fstream>
#include "math.h"

using namespace System;

void make_quark_masses();
double compute_answer(double);
double compute_value(double);
double Gamma(double);
double Z(double);

const int Flag = 3;
// Flag = 0 to graph unprocessed momentum space QCD spectral running coupling
// Flag = 1 to graph spectral QCD running coupling vs. energy unconstrained by CERN da
// Flag = 2 to graph spectral QCD running coupling vs. energy constrained by CERN data
// Flag = 3 to compare CERN data with spectral QCD running coupling,

const double Lambda = 1.4e1; // in GeV;
double alpha_b_0 = 1.0; // initial bare coupling for cases 2 and 3
double alpha_b = 1.0; // bare coupling for cases 0 and 1

double c, d;
double* mass;
double m;
double* tau_data;
double* alpha_data;
int n_data;
double offset;

const double pi = 4.0 * atan(1.0);
const double Lambda_display = 1.0e3;
const int n_display = 10000;
const double delta_display = Lambda_display / n_display;
const double factor = 8.065543937e5; // factor to convert from eV to m^{-1}
const double equivalent_length = 1.0 / (1.0e9 * Lambda * factor);

```

```

const int n_int_rho = 200;
const int n_int_xi = 200;
const int n_iter = 20;
const double delta_int_rho = Lambda / n_int_rho;
const double High_energy = 1.0e5;

int main(array<System::String>^ args)
{
    std::ofstream outFile("out.txt");

    std::cout << "Length equivalent to energy cutoff = " << equivalent_length << " m\n";
    make_quark_masses();
    offset = compute_value(High_energy);
    int i;
    if (Flag == 2 || Flag == 3)
    {
        std::ifstream inFile("sorted_data.txt");
        inFile >> n_data;
        std::cout << "n_data = " << n_data << "\n";
        tau_data = new double[n_data];
        alpha_data = new double[n_data];
        for (i = 0; i < n_data; i++)
        {
            inFile >> tau_data[i] >> alpha_data[i];
        }
        alpha_b = alpha_b_0;
        for (i = 0; i < n_iter; i++)
        {
            d = -(alpha_data[0] - alpha_data[n_data-1]) / (compute_value(tau_data[0]))
            std::cout << "alpha_b = " << alpha_b << " d = " << d << "\n";
            alpha_b = d;
        }
        c = alpha_data[n_data-1] + alpha_b * compute_value(tau_data[n_data-1]);
    }
    if (Flag == 3)
    {
        for (i = 0; i < n_data; i++)

```

```

        {
            double tau = tau_data[i];
            double answer = compute_answer(tau);
            outFile << log(tau) / log(10.0) << '\t' << answer << '\t' << alpha_data[i]
        }
    }
else if ((Flag == 0) || (Flag == 1) || (Flag == 2))
{
    for (i = 1; i < n_display; i++)
    {
        double tau = i * delta_display;
        double answer = compute_answer(tau);
        outFile << log(tau) / log(10.0) << '\t' << answer << "\n";
    }
}
else
{
    std::cout << "Invalid Flag\n";
    exit(1);
}
return(0);
}

double compute_answer(double tau)
{
    double v;
    if (Flag == 0) return(Gamma(tau));
    else if (Flag == 1) return(fabs(compute_value(tau) - offset));
    else return(-alpha_b * compute_value(tau) + c);
}

double compute_value(double tau)
{
    double answer = 0.0;
    int i, j;
    for (i = 1; i < n_int_rho; i++)
    {

```



```

        double rho = i * delta_int_rho;
        double xi_integral = 0.0;
        double delta_int_xi = rho / n_int_xi;
        for (j = 1; j < n_int_xi; j++)
        {
            double xi = j * delta_int_xi;
            xi_integral += Gamma(xi);
        }
        xi_integral *= delta_int_xi;
        answer += xi_integral * rho * sin(rho / tau);
    }
    answer *= delta_int_rho;
    answer /= (2.0 * pi * pi * pi);
    answer *= tau;
    return(answer);
}

```

```

void make_quark_masses()
{
    mass = new double[6];
    // masses in MeV
    mass[0] = 2.3; // up quark
    mass[1] = 4.8; // down quark
    mass[2] = 95.0; // strange quark
    mass[3] = 1275.0; // charm quark
    mass[4] = 4180.0; // bottom quark
    mass[5] = 173210.0; // top quark
    // convert to GeV
    int i;
    for (i = 0; i < 6; i++) mass[i] /= 1.0e3;
}

```

```

double Gamma(double Q)
{
    double answer = 0.0;
    int k;
    for (k = 0; k < 6; k++)

```

```

{
    m = mass[k];
    if (Q > (2 * m))
        answer += m * m * m * Z(Q) * (3.0 + 2.0 * Z(Q) * Z(Q)) / (Q * Q * Q); // f
}
answer /= -1.0 / (3.0 * pi);
answer += 19.0 / (32.0 * pi);
answer *= 4.0 * pi * alpha_b;
answer += 1.0;
return(answer);
}

double Z(double s)
{
    if (s < 2.0 * m)
    {
        std::cout << "error in Z function\n";
        exit(1);
    }
    double answer = sqrt(s * s / (4.0 * m * m) - 1.0);
    return(answer);
}

```